

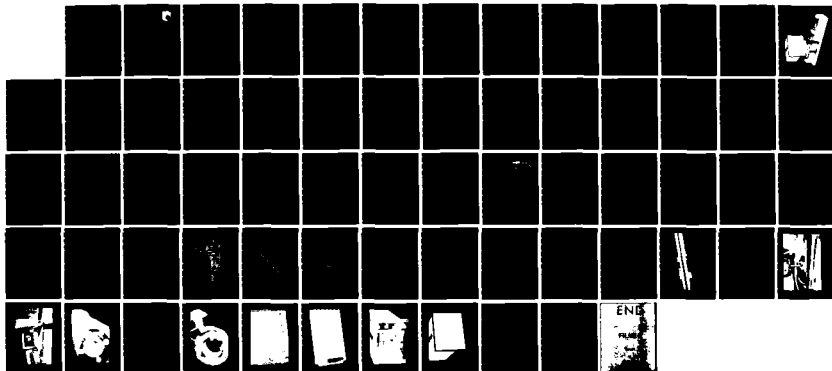
1/1

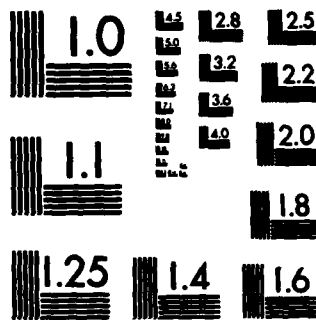
UNCLASSIFIED

F33615-82-C-3605

F/G 1/3

NL





MICROCOPY RESOLUTION TEST CHART  
NATIONAL BUREAU OF STANDARDS-1963-A

AFWAL-TR-84-3043



**A DIGITAL LINEAR POSITION SENSOR FOR FLIGHT  
CONTROL ACTUATION**

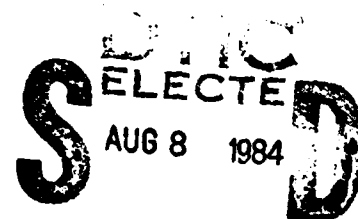
Gavin D. Jenney

Harry W. Schreadley

DYNAMIC CONTROLS, INC.

DAYTON, OHIO 45424

May 1984



Final Report for Period June 1982 - September 1983

Approved for public release; distribution unlimited.

FLIGHT DYNAMICS LABORATORY  
AIR FORCE WRIGHT AERONAUTICAL LABORATORIES  
AIR FORCE SYSTEMS COMMAND  
WRIGHT-PATTERSON AIR FORCE BASE, OHIO 45433

84 08 07 051

AD-A144 283

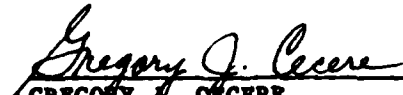
DTIC FILE COPY


# NOTICE

When Government drawings, specifications, or other data are used for any purpose other than in connections with a definitely related Government procurement operation, the United States Government thereby incurs no responsibility nor any obligation whatsoever; and the fact that the Government may have formulated, furnished or in any way supplied the said drawings, specifications, or other data, is not to be regarded by implication or otherwise as in any manner licensing the holder or any other person or corporation, or conveying any rights or permission to manufacture use, or sell any patented invention that may in any way be related thereto.


This report has been reviewed by the Office of Public Affairs (ASD/PA) and is releasable to the National Technical Information Service (NTIS). At NTIS, it will be available to the general public, including foreign nations.

This technical report has been reviewed and is approved for publication.

  
GREGORY J. CECERE  
Program Manager

  
EDWARD H. FLINN, Chief  
Control Systems Development Branch  
Flight Control Division

FOR THE COMMANDER

  
JAMES D. LANG, Col, USAF  
Chief, Flight Control Division  
Flight Dynamics Laboratory

"If your address has changed, if you wish to be removed from our mailing list, or if the addressee is no longer employed by your organization please notify AFWAL/FIGL, W-PAFB, OH 45433 to help us maintain a current mailing list".

Copies of this report should not be returned unless return is required by security considerations, contractual obligations, or notice on a specific document.

| REPORT DOCUMENTATION PAGE  |                                      | READ INSTRUCTIONS<br>BEFORE COMPLETING FORM   |
|--|--------------------------------------|---|
| 1. REPORT NUMBER<br>AFWL-TR-84-3043  | 2. GOVT ACCESSION NO.<br>N/A A144283 | 3. RECIPIENT'S CATALOG NUMBER<br>N/A  |
| 4. TITLE (and Subtitle)<br>A DIGITAL LINEAR POSITION SENSOR FOR FLIGHT<br>CONTROL ACTUATION  |                                      | 5. TYPE OF REPORT & PERIOD COVERED<br>Final<br>June 1982 - September 1983               |
|  |                                      | 6. PERFORMING ORG. REPORT NUMBER  |
| 7. AUTHOR(s)<br>Gavin D. Jenney<br>Harry W. Schreadley   |                                      | 8. CONTRACT OR GRANT NUMBER(s)<br>F33615-82-C-3605                                      |
| 9. PERFORMING ORGANIZATION NAME AND ADDRESS<br>Dynamic Controls, Inc.<br>7060 Clifwood Place<br>Dayton, Ohio 45424   |                                      | 10. PROGRAM ELEMENT, PROJECT, TASK<br>AREA & WORK UNIT NUMBERS<br>Project No. 2403-0286 |
| 11. CONTROLLING OFFICE NAME AND ADDRESS<br>Flight Dynamics Laboratory<br>Air Force Wright Aeronautical Laboratories<br>Air Force Systems Command<br>Wright Patterson Air Force Base, Ohio 45433  |                                      | 12. REPORT DATE<br>May 1984   |
| 14. MONITORING AGENCY NAME & ADDRESS (if different from Controlling Office)  |                                      | 13. NUMBER OF PAGES<br>65   |
|  |                                      | 15. SECURITY CLASS. (of this report)<br>Unclassified                                    |
|  |                                      | 15a. DECLASSIFICATION/DOWNGRADING<br>SCHEDULE   |
| 16. DISTRIBUTION STATEMENT (of this Report)<br><br>Approved for Public Release; distribution unlimited   |                                      |   |
| 17. DISTRIBUTION STATEMENT (of the abstract entered in Block 20, if different from Report)   |                                      |   |
| 18. SUPPLEMENTARY NOTES<br><br>None  |                                      |   |
| 19. KEY WORDS (Continue on reverse side if necessary and identify by block number)<br>Digital Measuring System<br>Digital Position Measuring<br>Position Transducer<br>Digital Position Sensor<br>Digital Transducer   |                                      |   |
| 20. ABSTRACT (Continue on reverse side if necessary and identify by block number)<br><br>This report describes a digital position sensor using incremental encoding of a rod by using alternate washers of ferrous and nonferrous material. Sensors are mounted radially around the rod. The technique was successful. The report describes the theory, demonstration hardware and the test results. ↑ |                                      |   |

## FOREWORD

The effort described in this document was performed by Dynamic Controls, Inc. of Dayton, Ohio under Air Force Contract F33615-82-C-3605. The work under the contract was carried out in the Air Force Flight Dynamics Laboratory , Wright-Patterson Air Force Base Ohio. The work was administered by Mr. Gregory Cecere, AFWAL/FIGL Project Engineer.

This report covers work performed between June 1982 and September 1983. The technical report was submitted by the authors in January 1984.

The authors express their appreciation to Dynamic Controls, Inc. personnel Carl Allbright and Julie Minch for their contribution in fabricating the development hardware and Connie Graham for her contribution in the preparation of this report.



|                    |  |
|--------------------|--|
| Accession For      |  |
| NTIS GRA&I         | <input checked="checked" type="checkbox"/> |
| DTIC TAB           | <input type="checkbox"/>                   |
| Unannounced        | <input type="checkbox"/>                   |
| Justification      |  |
| By                 |  |
| Distribution/      |  |
| Availability Codes |  |
| Dist               | Avail and/or Special                       |
| A1                 |  |

## TABLE OF CONTENTS

| SECTION     |                                 | PAGE |
|-------------|---------------------------------|------|
| SECTION I   | INTRODUCTION SUMMARY            | 1    |
|             | <u>Introduction</u>             | 1    |
|             | <u>Summary</u>                  | 3    |
| SECTION II  | TECHNICAL APPROACH              | 5    |
|             | <u>Techniques Investigated</u>  | 5    |
|             | <u>Technique Developed</u>      | 14   |
|             | <u>Theoretical Calculations</u> | 14   |
|             | <u>Electronics Design</u>       | 21   |
| SECTION III | TEST RESULTS                    | 33   |
|             | <u>Test Procedure</u>           | 33   |
|             | <u>Recorded Results</u>         | 33   |
| SECTION IV  | HARDWARE DESCRIPTION            | 43   |
|             | <u>General</u>                  | 43   |
|             | <u>Specific</u>                 | 43   |
| SECTION V   | CONCLUSIONS & RECOMMENDATIONS   | 55   |
|             | <u>Conclusion</u>               | 55   |
|             | <u>Recommendations</u>          | 56   |

## LIST OF ILLUSTRATIONS

| Figure |   | PAGE |
|--------|---|------|
| 1      | Demonstration Unit .....                            | 4    |
| 2      | Cross Section of Actuator Rod .....                 | 6    |
| 3      | Sensor Techniques .....                             | 7    |
| 4      | Narrow Gap Transformer.....                         | 9    |
| 5      | Inductive Coil Sensor Electronics Block Diagram ... | 10   |
| 6      | Sensor Output vs. Washer Encoder .....              | 12   |
| 7      | Transformer Sensor Electronics Block Diagram .....  | 13   |
| 8      | Narrow Gap Sensor Control Reluctance Design .....   | 16   |
| 9      | Transformer Coil Assembly .....                     | 10   |
| 10     | Sensor Mechancial Assembly.....                     | 20   |
| 11     | Block Diagram Schematic - Position Sensor.....      | 22   |
| 12     | 4X Logic Operation.....                             | 23   |
| 13     | 8X Logic Operation.....                             | 25   |
| 14     | Signal conditioner.....                             | 27   |
| 15     | Logic Pulse Generation Circuit.....                 | 28   |
| 16     | DC Offset Compensator.....                          | 30   |
| 17     | Up/Down Counter Schematic.....                      | 32   |
| 18     | Sensor Output Waveform.....                         | 35   |
| 19     | Sensor Output DC Shift.....                         | 36   |
| 20     | 4X Output Linearity without DC Tracking.....        | 37   |
| 21     | 4X Output Linearity with DC Tracking.....           | 38   |
| 22     | 4X Expanded Plot with DC Tracking.....              | 40   |
| 23     | 8X Output Linearity.....                            | 41   |



|    |   |    |
|----|---|----|
| 24 | 8X Expanded Plot.....                               | 42 |
| 25 | Encoded Shaft Closeup View.....                     | 44 |
| 26 | Narrow Gap Transformer Sensor & Encoded Shaft.....  | 46 |
| 27 | Sensor Sensitivity Test Setup.....                  | 47 |
| 28 | Sensor Ring Assembly - End View.....                | 48 |
| 29 | Sensor Mount.....                                   | 50 |
| 30 | Position Sensor Transformer Primary Circuit Card... | 51 |
| 31 | Position Sensor Secondary Circuit Card.....         | 52 |
| 32 | Position Sensor Electronics Unit - Internal View... | 53 |
| 33 | Position Sensor Electronics Unit.....               | 54 |

### List of Abbreviations and Symbols

|       |                      |
|-------|----------------------|
| $A_n$ | Cross Section Area   |
| BCD   | Binary Coded Decimal |
| cm    | Centimeter           |
| d     | depth                |
| $F_e$ | Iron                 |
| Fero  | Ferrous              |
| Hz    | Hertz                |
| I     | Current              |
| IC    | Integrated Circuit   |
| $l_n$ | Length               |
| in.   | Inches               |
| $L_n$ | Length               |
| N     | Number of Turns      |
| $R_n$ | Reluctance           |
| usec. | Micro Seconds        |
| $U_n$ | Relative Permability |
| v     | Volts                |
| W     | Width                |
| O     | Flux                 |

SECTION I  
INTRODUCTION AND SUMMARY

Introduction

The use of digital electronics in flight control systems has led to considering alternate techniques for creating the electrical signals by control system sensors. This report describes a unique linear position measurement sensor. Typical application for the sensor is measurement of the output displacement of linear actuators used in flight control systems.

The technique investigated is based upon incremental encoding of an actuator rod by using alternate layers of ferrous and nonferrous material in the construction of the rod. To detect the presence or absence of the ferrous material, sensors designed using transformer theory are mounted radially around the rod. The sensors are used to create an electrical change in state from high to low as the material presented to the sensor changes. A counter is used to keep track of the state changes in order to provide an output signal proportional to the position of the rod relative to sensors. Two sensors and a logic circuit are required to determine the direction of motion. This type of incremental encoding requires that an initial value be loaded into the counter (with the encoded rod at a predetermined specified position) to achieve absolute position measurement.

The advantages of the technique investigated are the following:

1. The sensor technique produces a digital output that can be interfaced easily with the digital electronics used in the control system.

2. The incremental encoding of the actuator rod is permanent and requires no configuration change for the actuator piston and rod.

3. The sensor components can be mounted internal to the actuator and be well protected from damage.

4. The encoding of the actuator rod extends around the circumference of the rod, allowing simple addition of more sensors in order to meet control system redundancy requirements.

5. The sensor technique is based upon inductive sensing which is compatible with operation in oil and in the contamination environment existing inside a linear hydraulic actuator.

6. The position measuring technique is not limited to hydraulic actuators and can be applied to other linear position sensing applications.

7. The sensor electronics operate with DC supply voltages, eliminating the requirement to provide AC power to the actuator (as with the linear variable differential transformers normally used in flight control actuator position measurement).

8. The electronics used with the sensor incorporate circuits and components which are adaptable to VLSI electronic packaging technology.

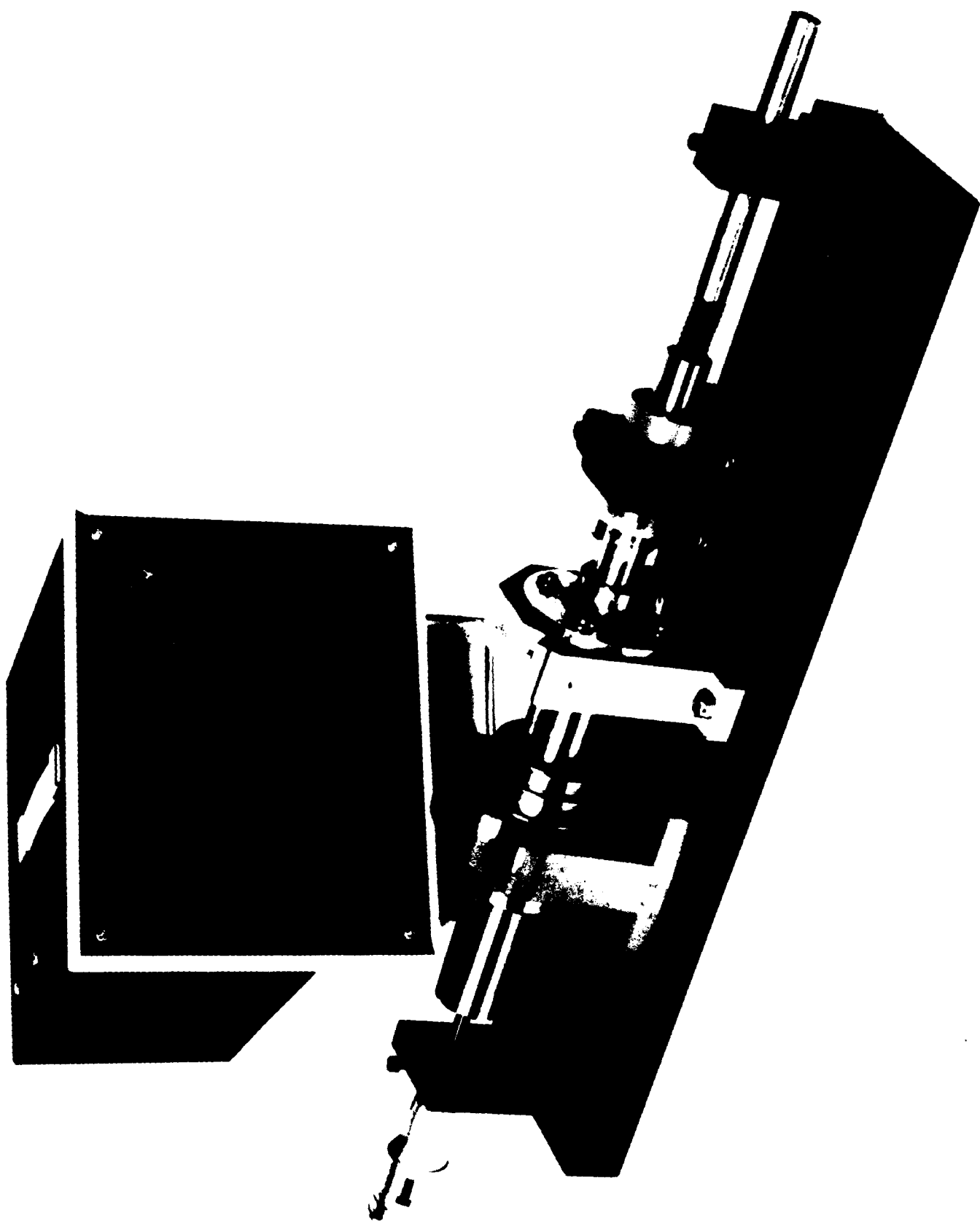
### Summary

A demonstration unit of the approach was fabricated and evaluated. The demonstration unit verified the feasibility. The design of the sensing heads used with the encoded rod were based upon transformer design, with the encoded rod material varying the coupling between the transformer's input and output windings. The measured sensitivity of the sensors was less than the sensitivity predicted by design calculations. The electronics used with the sensors for counting and direction determination are similar to that used with optical encoding sensors. Circuitry to compensate for small changes in the coupling efficiency over the length of the encoded shaft was included in the electronics.

The resolution achieved with the demonstration unit was 0.0025 in. This was obtained with a rod encoded with alternating layers of copper and steel having a thickness of 0.010 in. There is potential for achieving better resolution with sensors having smaller gaps and pole faces and used in combination with thinner layers of encoding material.

The investigation proved feasibility for the approach. Further development of the technique, particularly in the area of improving the sensitivity of the sensing head, is necessary before general application of the technique can be recommended.

Figure 1 shows the demonstration unit fabricated and evaluated for the work effort.



## SECTION II

### TECHNICAL APPROACH

#### Techniques Investigated

During the development of the demonstration unit, several sensor head techniques were designed and evaluated empirically. All sensor techniques were evaluated with the same encoded shaft (encoded with .010 in. thick alternating washers brass and steel as shown in Figure 2). The sensor techniques evaluated included two transformer coupling and one inductive coupling method.

The first technique (Figure 3) is based upon the concept of sensing an induction change of a sensing coil when the coil is placed in proximity with a metallic mass. The sensing coil is used as the inductor in the tank circuit of an oscillator. The oscillator frequency changes with coil inductance and is used to generate an output in the electronics used with the oscillator. A copper plate is placed across the face of the coil to act as an electrostatic shield. The copper plate uses a slit window to allow the coil field to appear on the other side of the plate in a limited area.

The second technique (Figure 3) is based upon the concept of using an open "C" frame transformer. The coupling between the primary and secondary windings change with the insertion of ferrous material between the open ends of the "C". By making a transformer with a frame having "C" faces similar in thickness to the ferrous washers used in encoding the shaft, the amplitude of the output of the secondary winding varies with a change of material between the "C" faces (when the primary winding is excited with a constant signal).

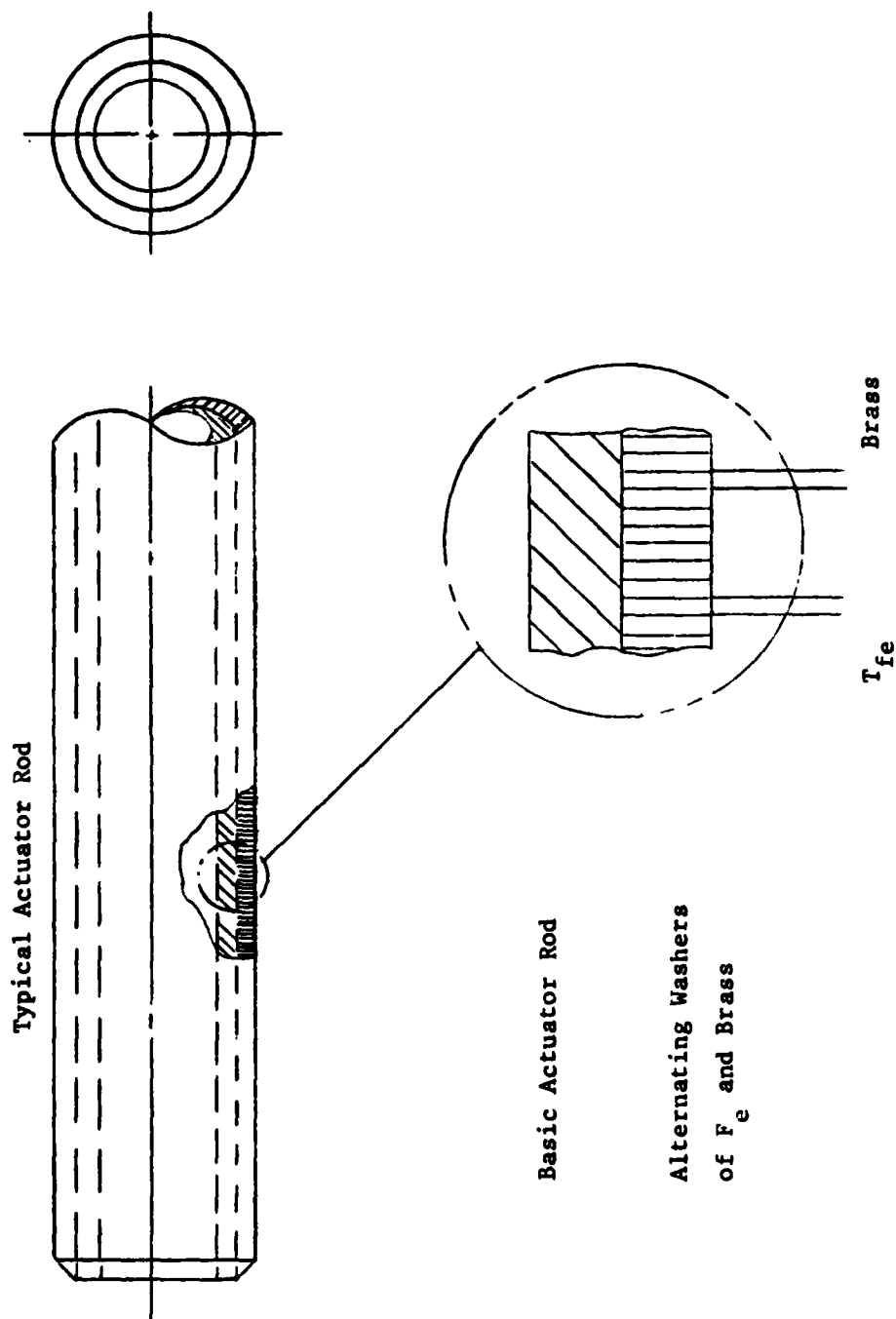
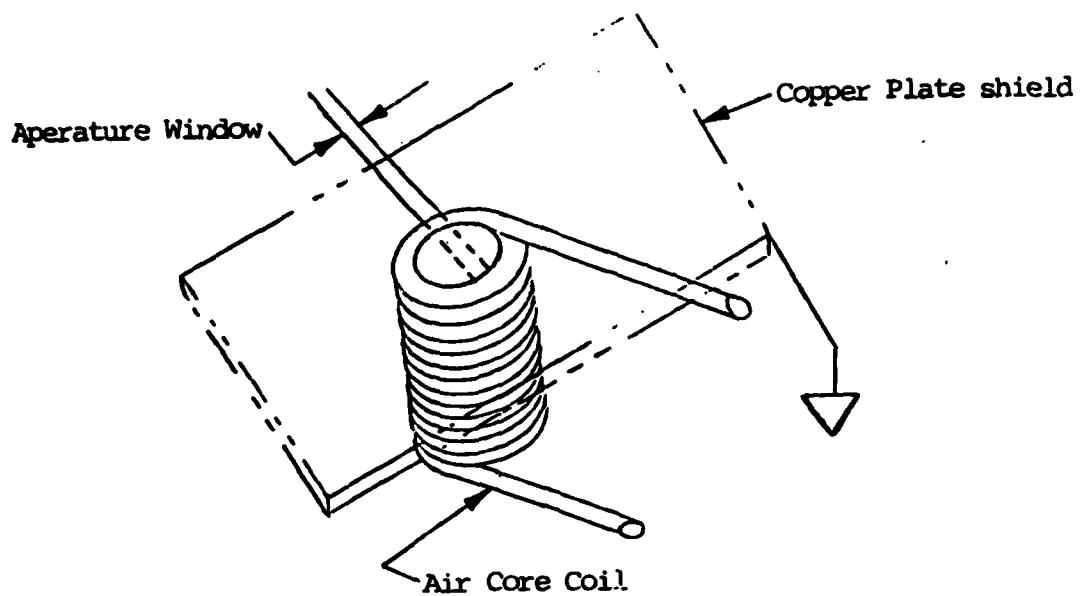
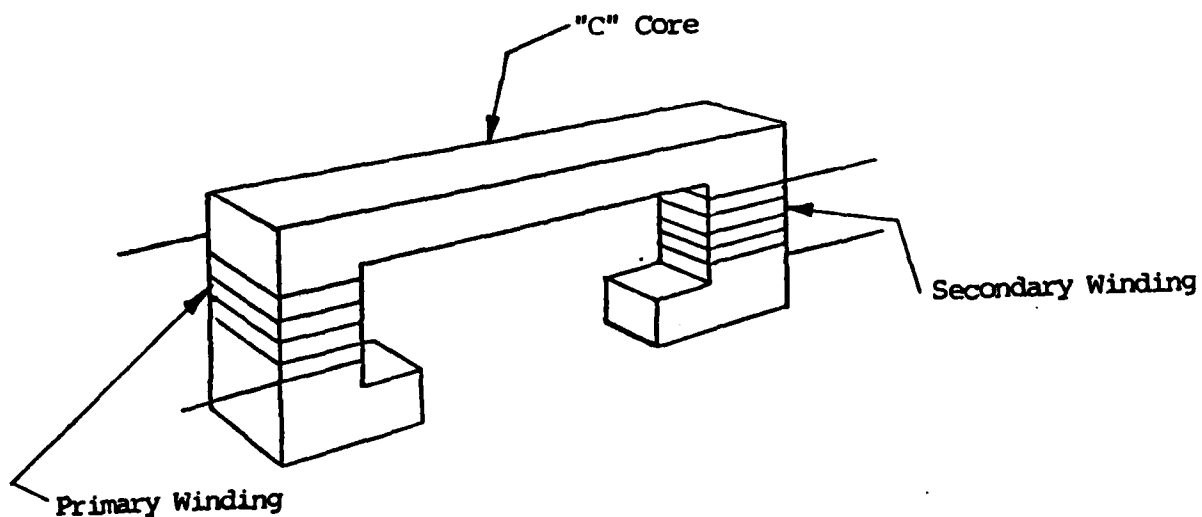


Figure 2 Cross Section of Actuator Rod





Inductive Coil Sensor



"C" Core Transformer Sensor

Figure 3 Sensor Techniques

The third technique (Figure 4) is based on the concept of a narrow gap transformer. The gap of the transformer is less than the width of the washers used to encode the shaft. The coupling of the secondary to primary windings is changed with the change of material at the gap of the transformer.

The cores of the "C" frame transformer and the narrow gap transformer were fabricated from sheets of Magnesil 0 electrical steel, .004 in. thick, a product of the Speciality Metals Division of the Magnetics Company. This construction was used to allow primary winding excitation frequencies of 10 KHz. With the transformer techniques, the excitation frequency establishes the maximum rate at which the shaft can move and the washers still be counted.

Figure 5 shows in schematic form the technique for creating the output change of state for the inductive coil sensor electronics. The detection circuit uses a phase locked loop single integrated circuit (IC) to create a voltage proportional to the frequency change of an oscillator circuit. The oscillator circuit uses the inductance of the sensing coil to determine its frequency of oscillation. The phase lock loop uses a voltage control oscillator to track the inductance controlled oscillator frequency. The phase lock loop IC has as one output the control voltage required to cause the phase lock loop to track the input frequency. In order to create a high or low state signal with the changing oscillator frequency, a comparator is connected to the control voltage output of the phase lock loop IC. The output of the comparator is used to drive a solid state switch connected to a suitable supply voltage, creating the high and low state output required for counting. Figure 5 also shows schematically the logic required for determining the direction of motion. Direction determination for the motion of the shaft requires two sensors, Offset to that

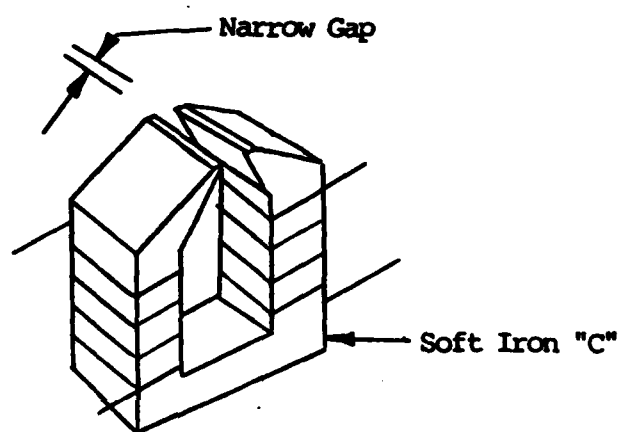


Figure 4. Narrow Gap Transformer

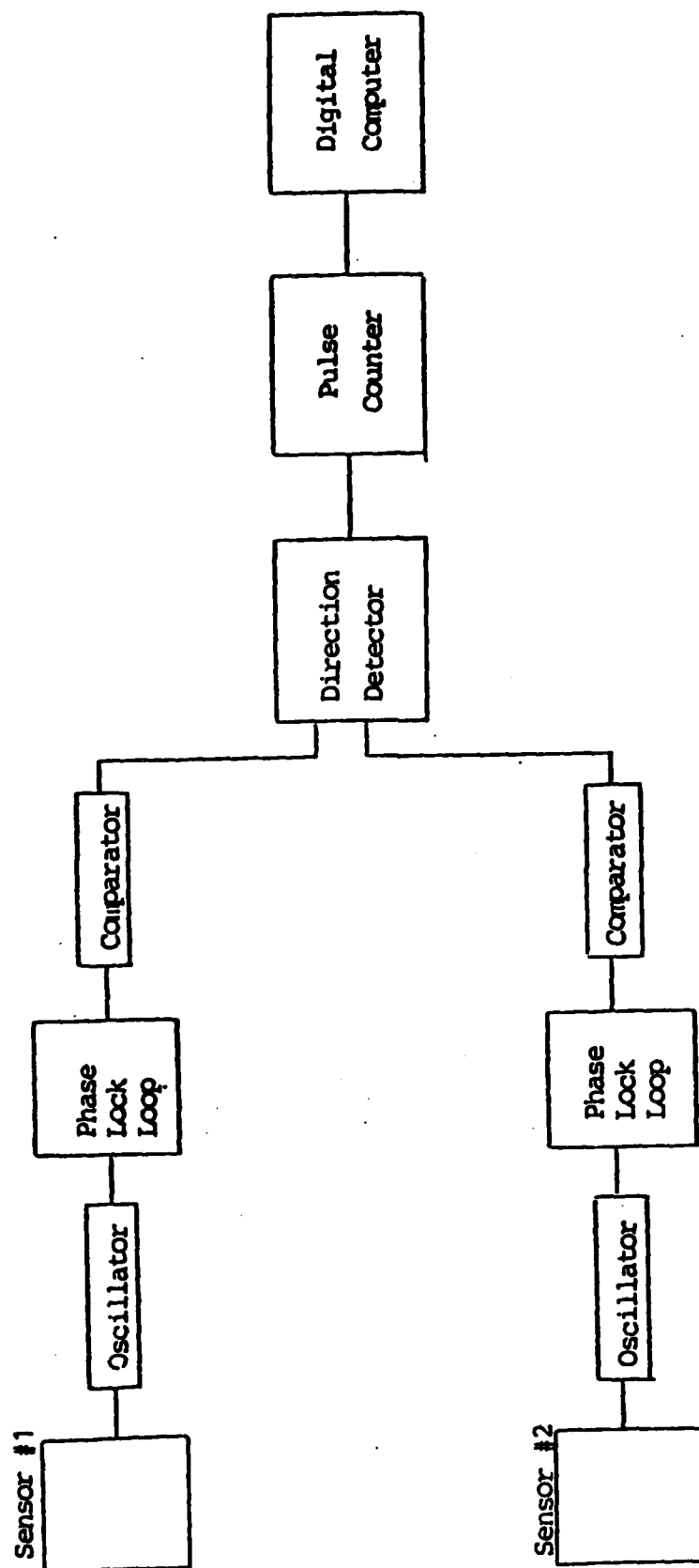


Figure 5 Inductive Coil Sensor Electronics Block Diagram

the change in the output of one sensor leads the other by one half of the spacing between the ferrous washers. Figure 6 illustrates the output of the two detection circuits connected to the direction sensing logic circuit. Note that knowing the state of one sensor output when the other changes is sufficient information to determine in which direction the shaft is moving. For example, if sensor 1 output goes from high to low, the direction of the shaft motion is to the left if the sensor 2 output was high during the sensor 1 transition. The motion of the shaft is to the right if sensor 2 output is low during the sensor 1 high to low transition. The output of the direction logic circuit is connected to an up-down counter to provide an output related to the shaft position.

Figure 7 shows in schematic form the electronics used with the transformer sensors. An oscillator is used to excite the primary windings of the sensors. As with the inductive coil technique, two sensors offset by one half the encoding washer thickness are used in order to provide direction sensing. The secondary windings outputs are rectified and filtered to provide a DC voltage. The DC voltages are amplified with gain stages and fed to comparators. The output of the comparators change state when the sensor outputs exceed and drop below the reference voltage used with each comparator. This creates an output state change which is counted in order to provide a value related to the shaft position.

The results of the three sensor technique investigation showed that the narrow gap sensor produced the largest output change when used with the encoded shaft. The percent change of inductance of the air coil with the slit window aperture and the percent change in the coupling of the primary to secondary winding of "C" transformer core configuration were both considerably less than that

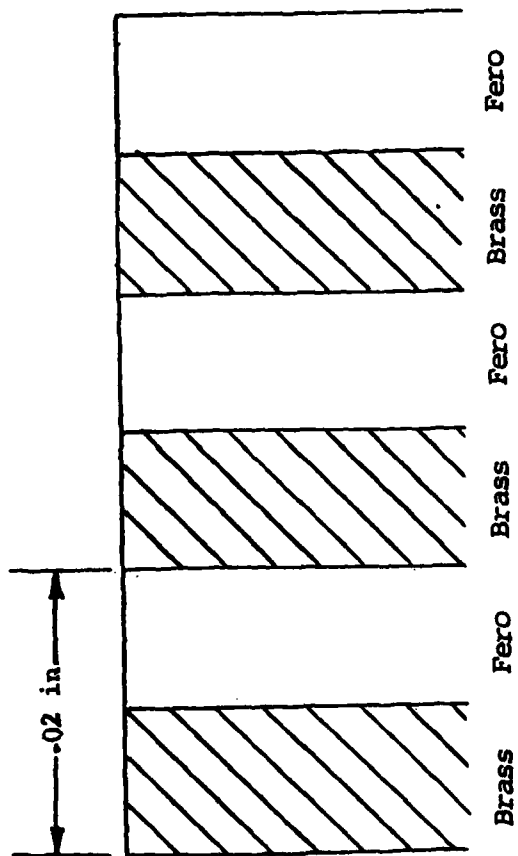
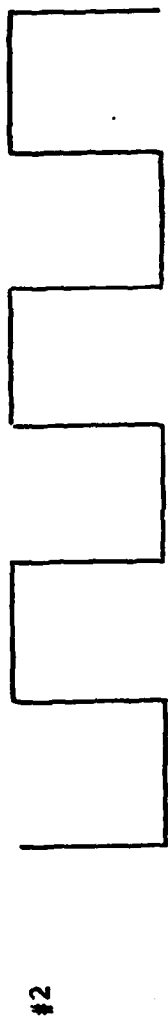
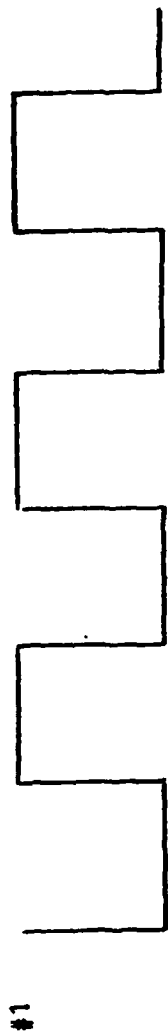


Figure 6. Sensor Output V.S. Washer Encoding

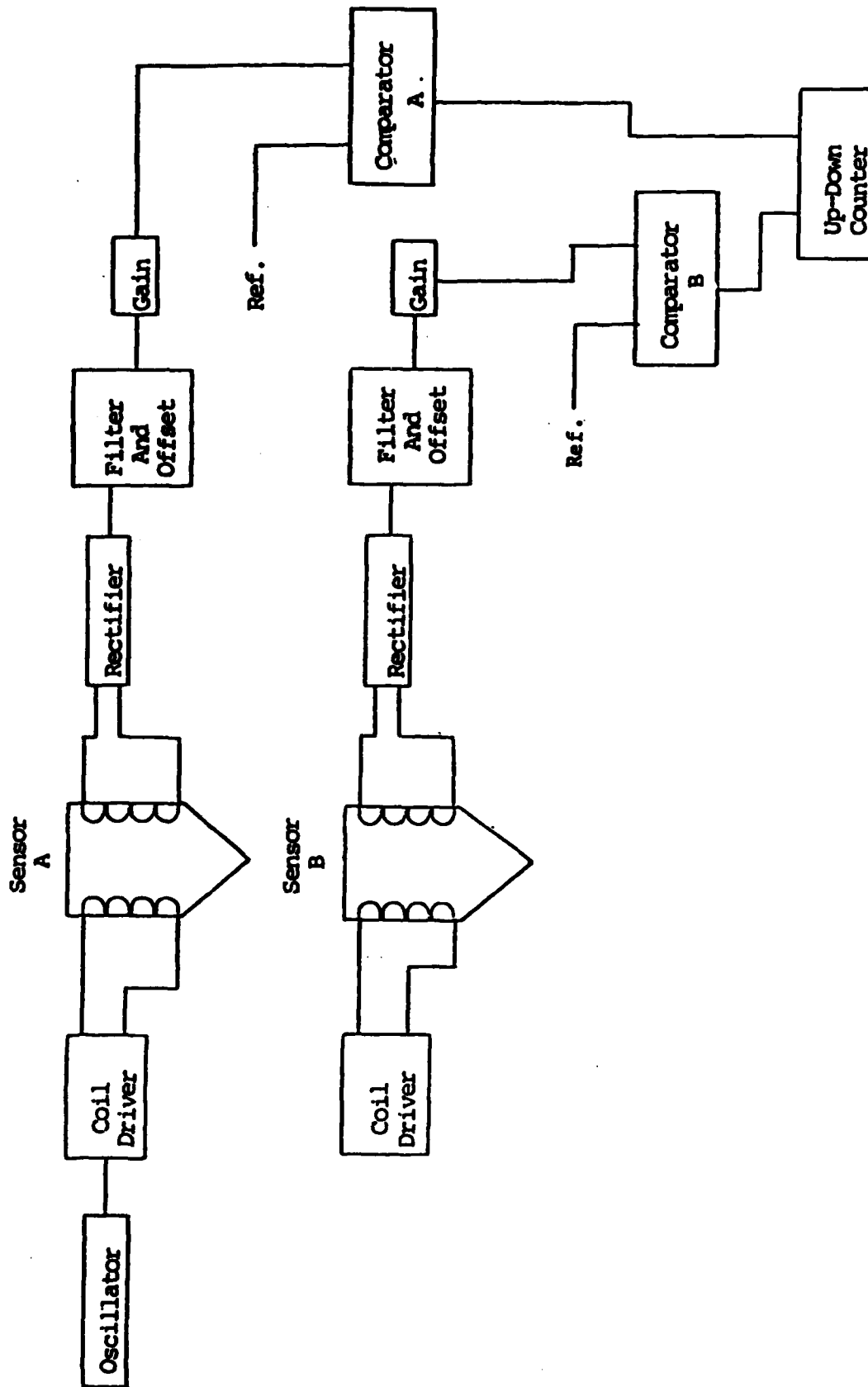


Figure 7. Transformer Sensor Electronic Block Diagram

measured with the narrow gap transformer design. The apparent reason for the low sensitivity for both these techniques was the tendency of the sensors to average the amount of ferrous material detected rather than selecting one washer at a time. The narrow gap transformer design concentrated the detection portion of the sensor in a smaller area and hence was able to detect individual washers as they were passed under the sensor.

### Technique Developed

The sensitivity check of the three sensing techniques indicated that the narrow gap transformer held the most promise. Therefore, this approach was developed further and used in the feasibility demonstration unit. No further work was expended on the other two techniques.

### Theoretical Calculations

The operation of the narrow gap transformer sensor is based upon transformer design equations. The magnetic circuit of a transformer is analogous to an electrical circuit in that the flux in the transformer core is proportional to the magnetomotive force "F" and inversely proportional to the reluctance "R" or magnetic resistance. Reluctances in series are added to obtain their combined reluctance. Ohm's law for a series magnetic circuit (expressed in the cgs system units) is:

$$\Phi = \frac{.4 \pi NI}{L_1/A_1U_1 + L_2/A_2U_2 + \dots + L_n/A_nU_n}$$

Where: .4 NI is the magnetomotive force in gilberts

$\Phi$  is in maxwells

$L_n, A_n, U_n$  are the lengths in cm, crosssection areas in  $\text{cm}^2$  and relative permeabilities in each series part of the circuit, respectively.



The narrow gap transformer design is based upon having one reluctance in the series circuit of the transformer core dominate the total reluctance and therefore flux in the transformer core for a given magnetomotive force. If the dominant reluctance is varied by the shaft encoding, then the flux in the transformer core also varies with the shaft encoding. By using a secondary winding on the transformer core, the change in flux in the core (with a constant ampere-turn input on the primary winding) can be measured as a secondary winding output voltage change. In the narrow gap sensor, an air gap is designed to be the dominant reluctance. The reluctance of the air gap is varied by moving the ferrous washers across the air gap. This changes the flux in the transformer core and the secondary winding output voltage.

Figure 8 shows schematically the narrow gap sensor with the control reluctance expanded for clarity at the bottom of the figure. For the narrow gap sensor evaluated, the dimensions of the control reluctance structure were:

$$l_1 = 0.003 \text{ in.}$$

$$l_2 = 0.001 \text{ in.}$$

$$l_3 = 0.003 \text{ in.}$$

$$d = 0.040 \text{ in.}$$

$$w = 0.010 \text{ in.}$$

Note that the sensor head width ( $l_1 + 2l_3$ ) @ .009 in. is slightly less than the width of the encoding washer (0.010 in.).

The change in gap reluctance with and without the encoding washer can be calculated as follows, letting  $R_1$  be the reluctance of the magnetic path across the pole pieces (without the encoding washer present) and  $R_2$  be the reluctance of the magnetic path from the pole pieces through the encoding washer:

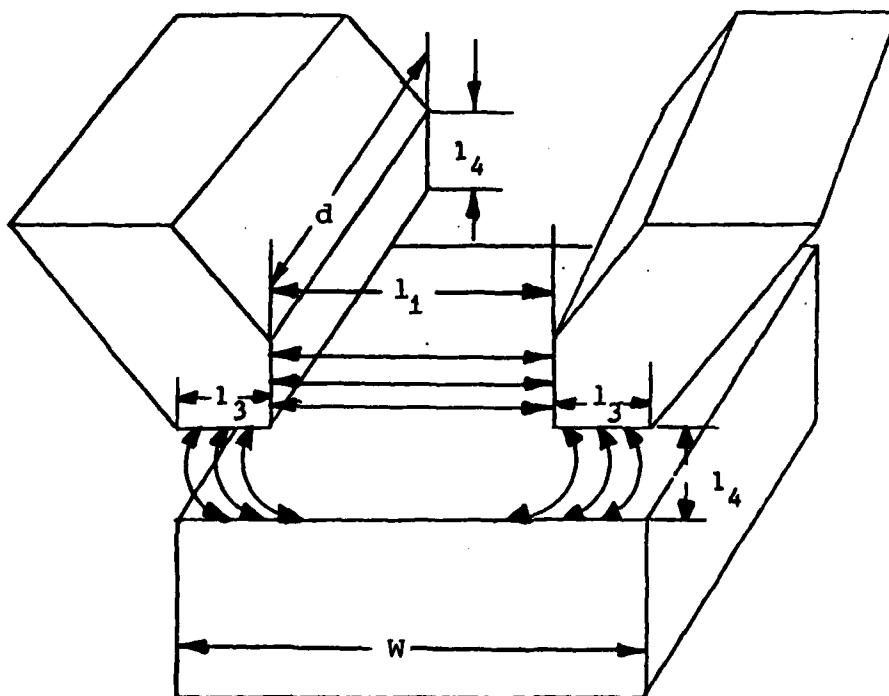
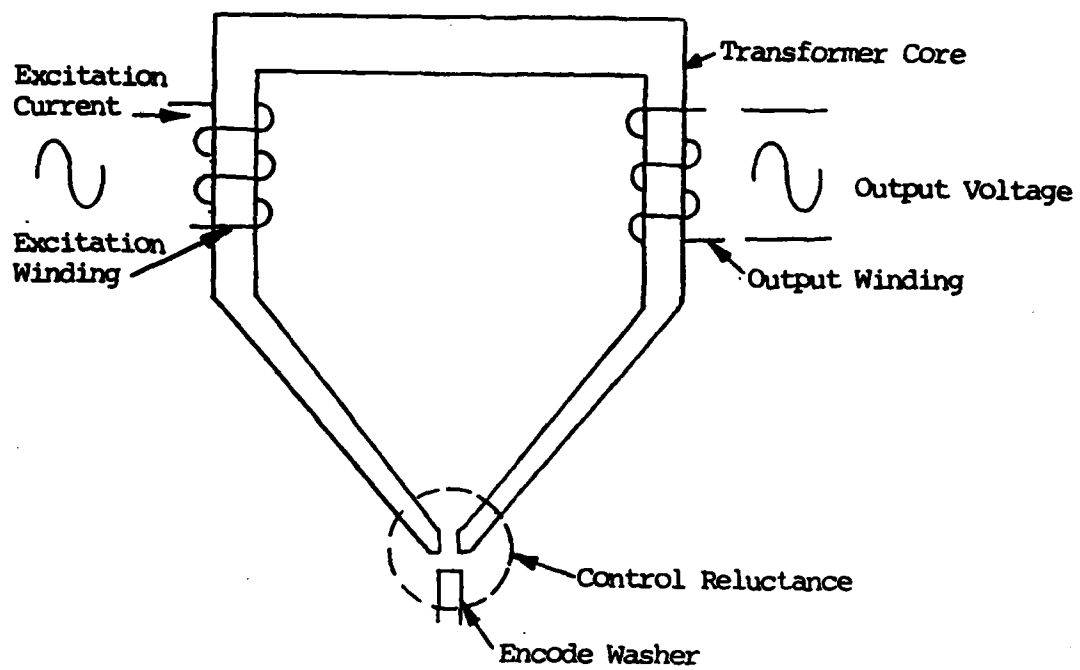


Figure 8. Narrow Gap Sensor Control Reluctance Design

$$R_1 = l_1/A_1U_1$$

Where for the cgs system  $U_1 = 1$

Substituting in the dimensional values used for the narrow gap sensor in units for the cgs system:

$$R_1 = (.003)(2.54)/(.003)(.040)(2.54)^2$$

$$R_1 = 9.843 \text{ gilbert/maxwell}$$

In the same way, with the washer in place:

$$R_2 = 2l_4/l_3d$$

Substituting in the values used for the narrow gap sensor in units of the cgs system:

$$R_2 = (.002)(2.54)/(.003)(.040)(2.54)^2$$

$$R_2 = 6.562 \text{ gilbert/maxwell}$$

Since  $R_1$  and  $R_2$  appear as parallel magnetic paths when an encoding washer is at the sensor gap, the gap reluctance is changed to  $R_{equiv}$ :

$$R_{equiv} = R_1R_2/R_1 + R_2$$

$$R_{equiv} = 3.937 \text{ gilbert/maxwell}$$

Therefore, the control gap reluctance changes from 3.937 with the encoding washer at the gap to 9.843 without the encoding washer. This is better than a two to one change in reluctance and theoretically should result in a corresponding change in the magnitude of the core transformer flux and secondary winding output voltage.

In order for the air gap of the transformer to control the flux in the transformer core, the rest of the transformer magnetic circuit must have a relatively low reluctance compared to the air gap. Figure 9 is the mechanical drawing for one half of the transformer core. Two of these halves are fastened together to form the sensor core, complete with the air gap. The A3 steel plates shown in Figure 9 are used to clamp the Magnesil-0 laminated core. Ten layers of Magnesil-0 sheet 0.004 in. thick are used for the transformer. At 10 KHz excitation current, the range of permeability of the Magnesil-0 is from 1250 to 6000 (corresponding to a flux of from 5 to 6000 gauss). The calculated value for the reluctance of the Magnesil-0 path (using an average width of the tapered sections of 0.085 in., an average length of the tapered sections of 0.33 in., a path length of 0.63 in. for the non-tapered portion of each half of the transformer, a "worst case" relative permeability of 1250 for the Magnesil-0) is:

$$R_I = 0.144 \text{ gilbert/maxwell}$$

This reluctance is considerably less than the lowest calculated reluctance for the control air gap ( $R_{equiv} = 3.937$ ). Therefore, the change in the reluctance of the air gap with and without the encoding washer should be the primary controller of the flux in the transformer with a constant ampere turn input. In addition, the effect of the flux level on the permeability of the Magnesil-0 can be ignored (with the constraint that the saturation flux of 6000 gauss is not exceeded).

Figure 10 is the mechanical assembly drawing for the narrow gap transformers mounted in position for the demonstration unit. Note that two transformer pairs are used for each sensor. The transformers for each pair are located



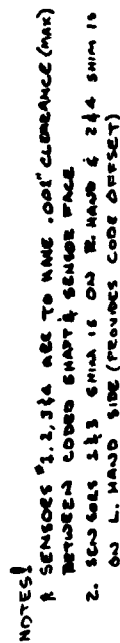


**Figure 10 Sensor Mechanical Assembly**

directly across from each other. By connecting the secondary windings of the transformer pairs in series with each other, the effect of variations in the clearance between the encoded shaft and the sensor gap due to shaft bearing clearances tend to be cancelled out.

### Electronics Design

Figure 11 is a block diagram schematic of the electronics used with the narrow gap transformer sensor. The schematic is similar to the general schematic of Figure 7 with the addition of an auto drift compensator, 8X bidirectional logic and the use of two transformers for each position sensor.

The demonstration unit was evaluated with both 4X and 8X bidirectional logic electronics. The 4X (the encoding washer thickness) resolution is inherent in using two position sensors in order to determine direction of motion. Figure 12 illustrates the 4X logic operation. The output of the position sensors are shown as a triangular waveform amplitude variation with position for illustration purposes (the actual sensor output is sinusoidal). As shown in Figure 12, the sensor output levels used to generate pulses for counting are the zero voltage output levels. For sensor A, these are points 1 and 3 on the waveform. For sensor B, these are points 2 and 4 on the output waveform. Figure 12 also shows the output of comparators which switch at the zero output level for the sensors. The comparator for sensor A (labeled 2A on Figure 12) goes high when the sensor output changes from a negative to positive value (point 1 on the Sensor A Output waveform) and goes low when the sensor A output again changes to a negative value (point 3 on the Sensor A Output waveform). Sensor B comparators generate similar level changes. Note that Figure 12 shows both the 2A and 2B comparator outputs and their complements.

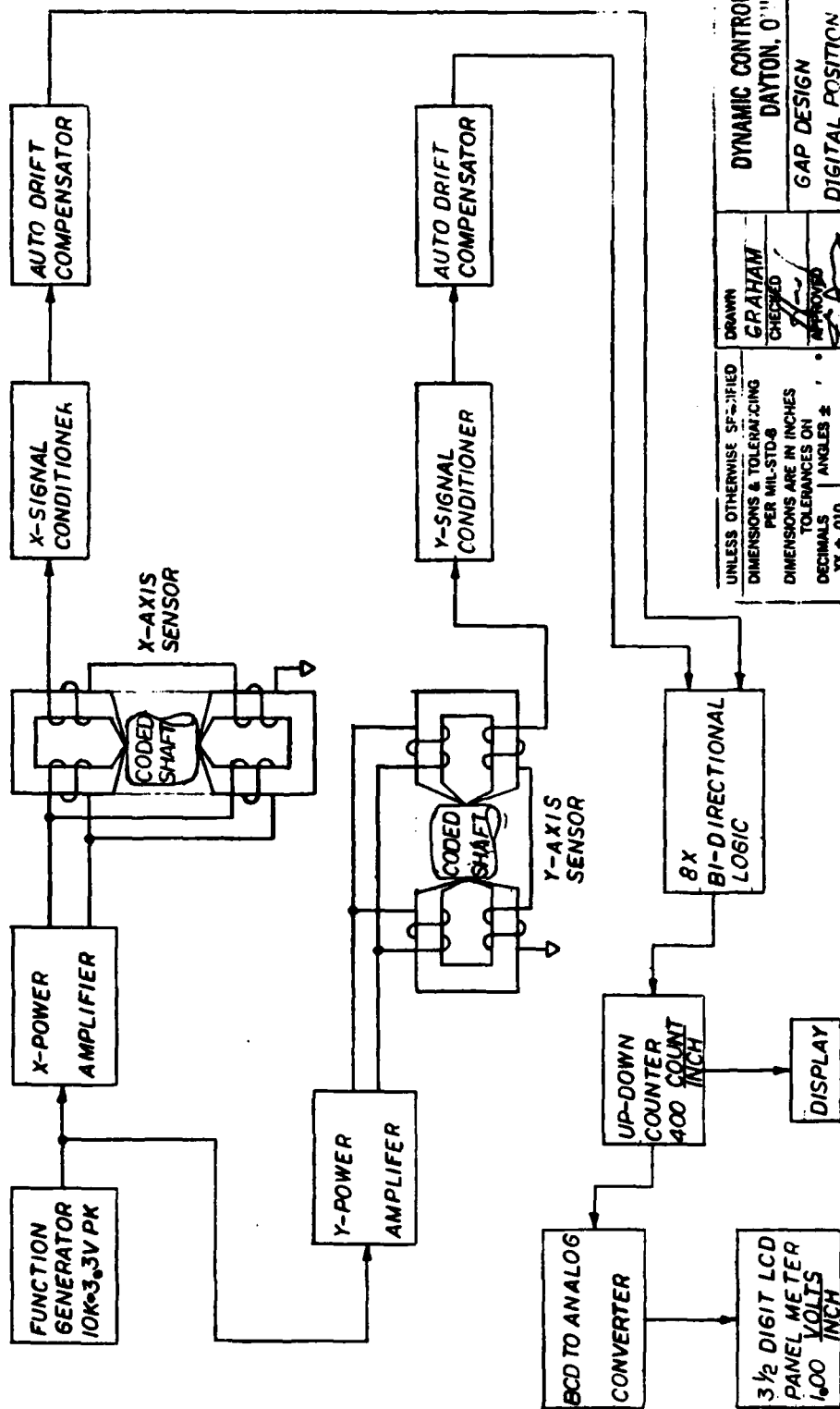


Figure 11 Block Diagram Schematic - Position Sensor

|   |  |                 |                         |    |
|---|--|-----------------|-------------------------|----|
| UNLESS OTHERWISE SPECIFIED<br>DIMENSIONS & TOLERANCING<br>PER MIL-STD-8 |  | DRAWN<br>GRAHAM | DYNAMIC CONTROLS, INC.  |    |
| DIMENSIONS ARE IN INCHES<br>TOLERANCES ON                               |  | CHECKED         | DAYTON, OHIO            |    |
| DECIMALS ANGLES FRACTIONS ±   |  | APPROVED        | GAP DESIGN              |    |
| XX ± .010<br>XXX ± .005   |  | DATE 8-84       | DIGITAL POSITION SENSOR |    |
| FINISH PER MIL-STD-10<br>✓ REMOVE ALL BURRS                             |  | DO NOT SCALE    | SCALE 15                | OF |
|   |  |                 | SHEET                   |    |



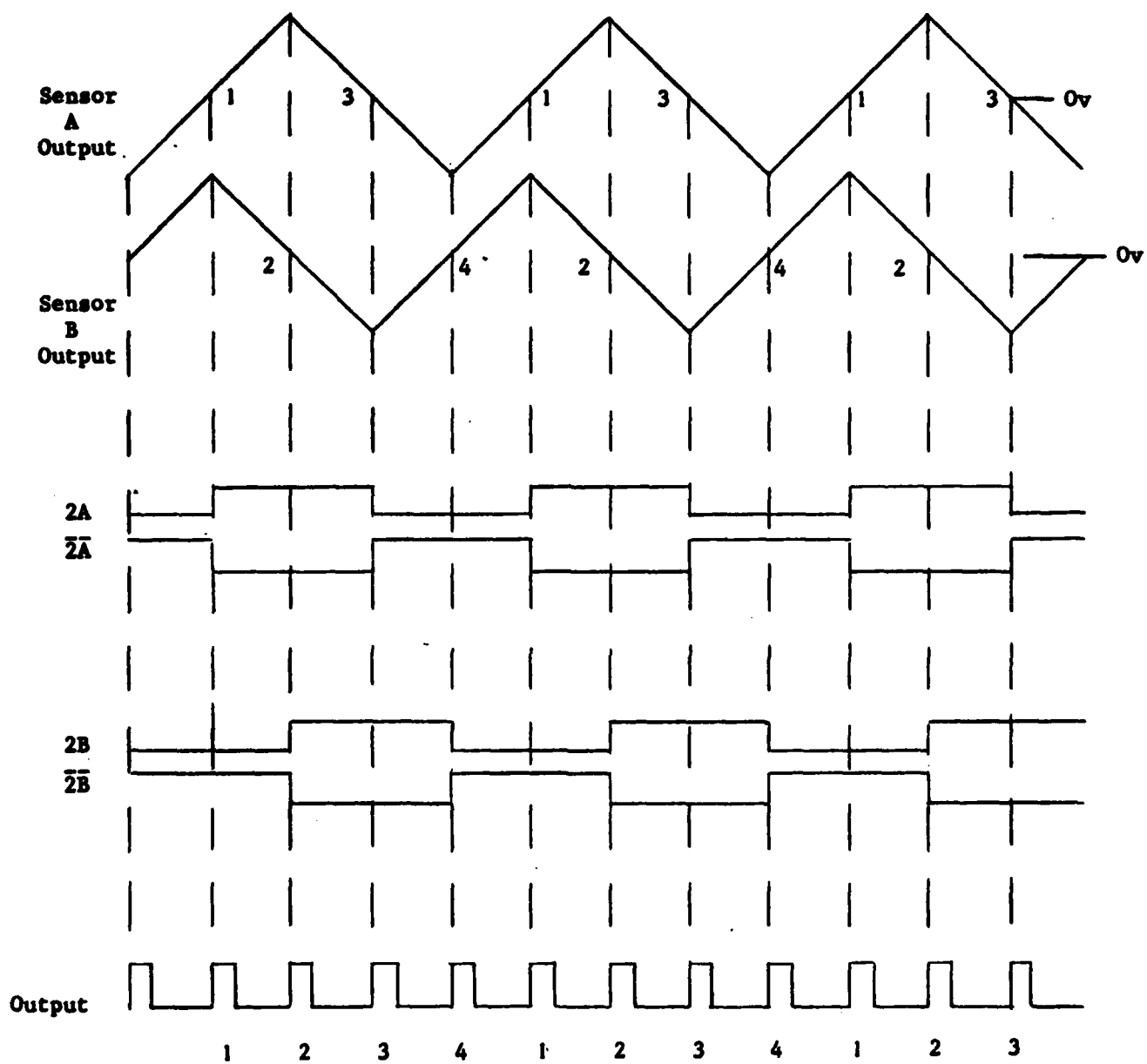


Figure 12 4X logic Operations

This is done because available IC logic elements require using "0" levels and negative transitions (going from high to low). For each pulse that is generated, the logic requires that two conditions exist - a "0" level on one line and a negative transition on another. Note that as shown in Figure 12, for motion generating pulses in order (1,2,3,4...etc.) there are four such unique conditions for each "cycle" (2B & 2A complement, 2A complement & 2B complement, 2B complement & 2A, 2A & 2B) which are used to generate 4 pulses. Note that for motion in this direction, the "0" state lines are 2B, 2A complement, 2B complement and 2A for pulses 1,2,3 & 4 respectively and the negative transition lines are 2A complement, 2B complement, 2A and 2B. For motion in the opposite direction (generating pulses 4,3,2, & 1) the "0" state lines are the same as for the other direction, but the negative transition lines are changed to 2B complement, 2A complement, 2B and 2A for pulses 4,3,2 & 1 respectively. This difference in the transition lines for the same "0" state is used to establish a direction of motion signal for the up-down counter. Figure 13 shows the 8X logic operation. This is a further division of the sensors output waveform by using comparators that detect predetermined sensor output levels as well as the transition from negative to positive output voltages. As shown on this figure, the "0" state and negative transition conditions are required (as with the 4X logic) for generation of a pulse. The voltage level points used for comparator inputs are shown as 1,2 and 3 on the output of Sensor A and Sensor B. Point 1 is a negative voltage level, point 2 is zero voltage and point 3 is a positive voltage. For example, for motion generating pulses 1 through 8 during one cycle, the corresponding negative transition lines are 2A complement, 3A complement, 2B, 3B, 2A, 1A, 2B, complement, 1A complement while the corresponding "0" state lines are 2B Complement, 2B complement, 2A complement, 2B, 2B, 2B, 2A and 2B complement. As

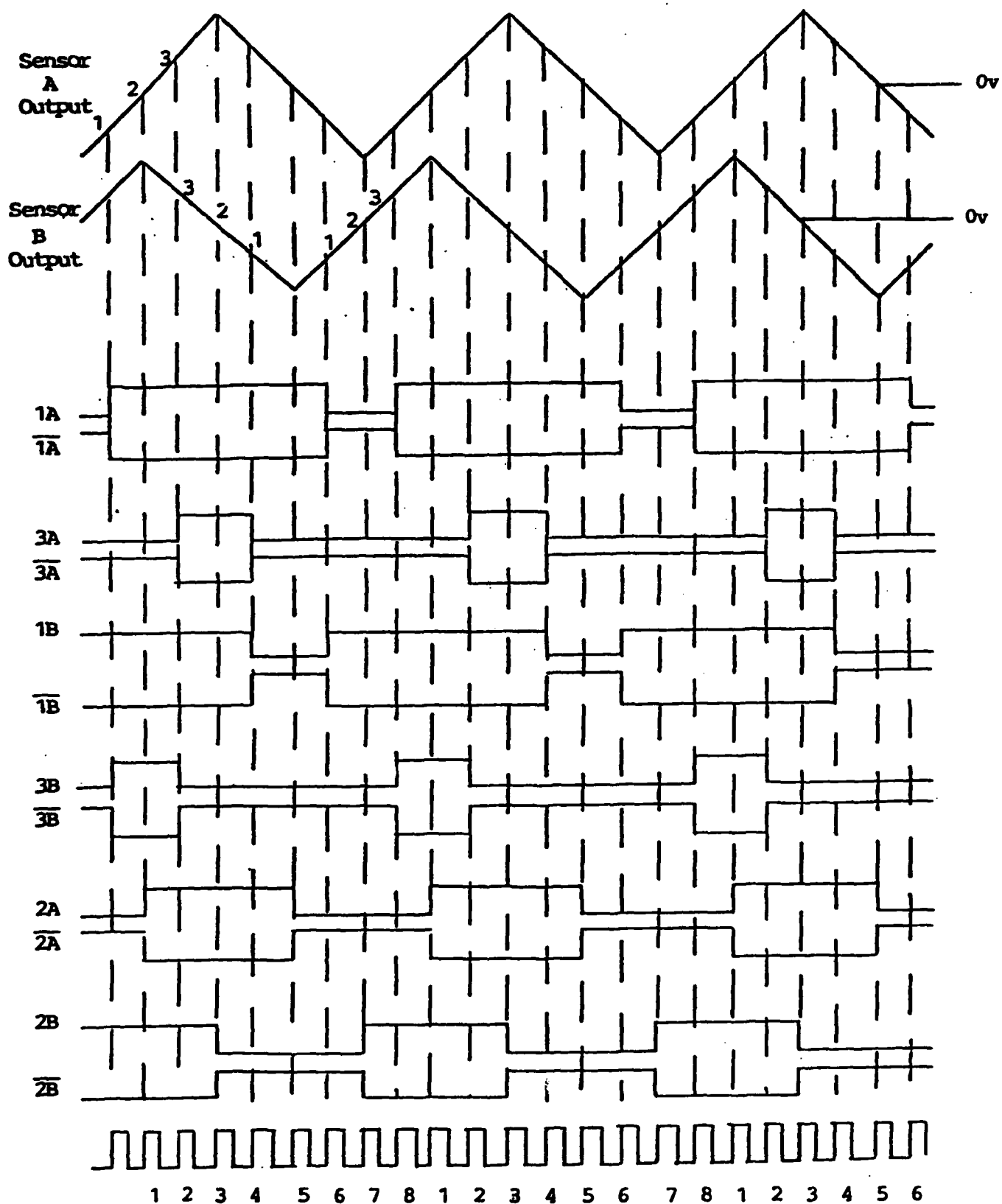


Figure 13 8X Logic Operation

with the 4X logic, the opposite direction of motion uses the same "0" state lines and different transition lines for the generation of the pulses.

Note that 1B, 1B complement, 3B and 3B complement are not used as transition lines in the generation of pulses. By using sensor A's output for most of the pulse generating negative transitions, the requirement for output waveform fidelity from both sensors is relaxed.

Figure 14 is the electrical schematic of the signal conditioner section of the electronics used with the narrow gap sensors. U-1 on Figure 14 generates the sinusoidal 10K Hz signal used to excite the primary windings of the narrow gap sensors. A-9 and A-10 are used to generate the necessary driving current for the primary windings. Driving voltages for the coils (300 turns of #38 AWG copper wire with an inductance of 4 mh and a resistance of 13 ohms) were 20 volts peak to peak. The output of the secondary windings (300 turns of #38 AWG copper wire) of the narrow gap are buffered with unity gain amplifiers A-1 and A-8. The nominal gain through the conditioning electronics is 40, required to amplify a 100 mv peak to peak sensor output signal variation to a level of 4 volts. The output of the sensors are demodulated using peak detection switches S-1 and S-2.

Figure 15 is the electrical schematic for the pulse generation and direction signal logic. Comparators U1-1,2 & 3 and U2-1,2 & 3 are used to generate the basic state changes corresponding to the different levels on the sensor output waveforms. U11-1 through U11-6 & U12-1 through U12-6 are used to generate the logic signals and their complements. Note that in order to limit noise intrusion and prevent level indecisions, U14,U15,U16 and U17 (which use Schmitt





trigger buffers) are used in the logic signal lines to generate pulses for the NOR gates. The NOR gates U3, U4, U5 & U6 use two inputs, one for reading the negative transition pulses on the logic lines and the other to read a "0" state condition on its logic lines. Note that U3 and U4 gates are connected to generate pulses for extend motion while U5 and U6 gates are connected to generate pulses for retract motions. U7-1, 2, 3 & 4 gather the extend (or retract) pulses for the circuitry which follows. NAND gates U10-1 and U10-2 are connected to drive a direction line for the digital counter. U10-3 drives U13 which provides a total pulse count for the digital counter and provides a necessary delay of 100 usec between the actual pulse generation and the pulse connected to digital counter. This delay is required in order to allow the digital counter time to process a change in the direction line before a count pulse is presented for processing.

Figure 16 is the electrical schematic of circuitry incorporated during the development program to compensate for DC shifts in the sensor output conditioned waveform. The DC shift in the waveform created false counts in the digital counter. The technique used to correct for the DC shifts was to use sample and hold circuitry to track and retain the  $\pm$  peak voltage levels for each sensor's output. The difference between the  $\pm$  peak voltage is divided by a ladder resistor network to obtain reference inputs for the comparators used to generate the state changes for the logic lines. As shown on Figure 16, U-1A & U-1B are solid state relays used to initialize and connect the sensor outputs to the peak detecting circuitry. For sensor A, sample & holds A-1 and A-3 retain the positive and negative peak voltages as the sensor output changes through each cycle. These voltages are transferred A-2 and A-4 sample & holds only after the sensor outputs have generated 8 pulses in one direction.

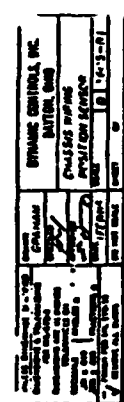




direction. For sensor A, resistors R14 through R17 divide the difference between the negative peak voltage and positive peak voltage retained by A-2 and A-4 sample & holds for use as comparator input reference voltages. Loading the A-2 and A-4 (for sensor A) occurs only after 8 extend or retract pulses have occurred, ensuring that a complete cycle has occurred. U-3 and U-4 counters count the extend and retract pulses, respectively. Both U-3 and U-4 counters are reset to zero when 8 pulses in either direction have occurred by the output of U7. These counters are also reset to zero if there is a change in the direction of motion, as detected by the retract and extend signal lines connected to U5 & U6 respectively.

The peak hold circuits are reset after 8 extend or retract pulses are counted. This is done by the output of U9 causing U-1A & U-1B to transfer to the reset position. This reset loads an initial value of 2.5 volts into the peak hold circuit. This voltage is within the range of the least positive peak value and the greatest minimum value of the input waveform and is then used by the peak hold circuit in determining whether to retain newly sampled  $\pm$  values.

Figure 17 is the interconnect schematic for the up/down counter, BCD to analog converter and the 3 1/2 digit digital voltmeter. As shown on the schematic, only two lines connect from the logic board to the up/down counter, one line (to pin 43 on the counter) being the pulse line and the other (to pin 41 on the counter) being the direction line.



32

## SECTION III

### TEST RESULTS

#### Test Procedure

The demonstration unit was designed so that a measured shaft displacement could be used to evaluate the performance of the narrow gap sensors and electronics. A micrometer head mounted at one end of the shaft was used to move the shaft to a known deflection. To allow electrically recording of the shaft motion (for comparison with the output of the sensor electronics), a precision potentiometer was attached to the encoded shaft at its other end. The narrow gap sensor was evaluated by moving the encoded shaft and recording the electrical output of interest.

#### Recorded Results

Figure 18 shows the output waveform of the narrow gap sensors. The general shape is that of a sinusoid (rather than a square wave). For a 4X (the washer thickness) output resolution, the waveform is unimportant. For a 4X sensor, a repeatable transition between maximum and minimum output signal levels (as each washer passes the gap) is all that is required. For the 8X application, there is a requirement for a gradual transition with displacement (such as a triangular or sinusoidal waveform). The gradual transition allows pulses to be generated reliably for several sensor output levels between the maximum and minimum output levels. The sensor output illustrated by Figure 18 show some "flattening" at the bottom. As measured on the 8X position linearity data, this waveform distortion limits the 8X configuration from reaching its theoretical resolution.

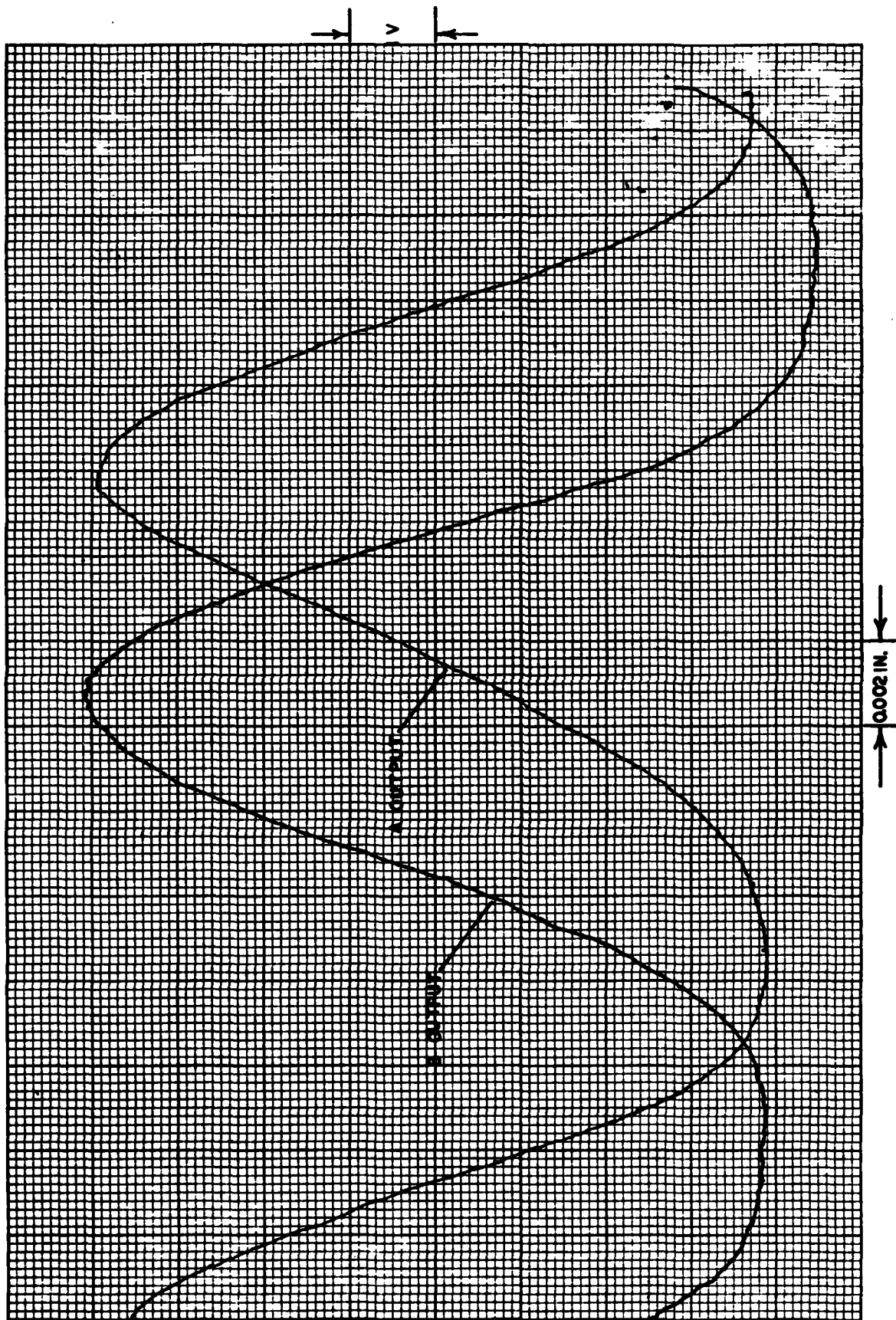


Figure 18 Sensor Output Waveform

Figure 19 illustrates the DC shift of the sensor outputs along the length of the encoded shaft. The DC shifts as shown on Figure 19 are on the order of 50% of the peak to peak output of the sensors. Although these DC effects perhaps could have been minimized by more pains taking fabrication of the sensor elements and electronics, that approach was not pursued. The technique used to deal with the shifts was to measure the DC shift of each sensor and cancel the effect out of the level sensing comparator operation. This technique potentially relaxes the requirement for expensive precision in the manufacture of the sensor and encoded shaft and allows some component variation without miscounting problems. The 4X technique can tolerate DC shifts of a magnitude nearly as great as the maximum sensor output. However, the 8X technique cannot. The automatic tracking of the DC shift is required for reasonable 8X operation.

Figure 20 shows the output of the sensor electronics vs. the coded shaft displacement for the 4X sensor electronics without DC tracking. The shaft displacement as measured by the position potentiometer is shown plotted on the horizontal axis, the analog output voltage from the BCD converter (ref. Figure 17) is plotted on the vertical axis. The plot is for 0.500 in. shaft deflection. Note that on the upper right of the plot, there is noticeable irregularity in the output of the sensor electronics. Figure 21 shows the output of the 4X sensor electronics vs. the coded shaft displacement with the DC tracking circuit (ref. Figure 16) installed. The irregularities in the output steps of the BCD to analog converter have essentially been eliminated. Note that on Figure 21 there are slightly less than 10 steps for each 0.050 in. of travel. This is due to the washer thicknesses being slightly greater than 0.010 in. when assembled on the shaft .

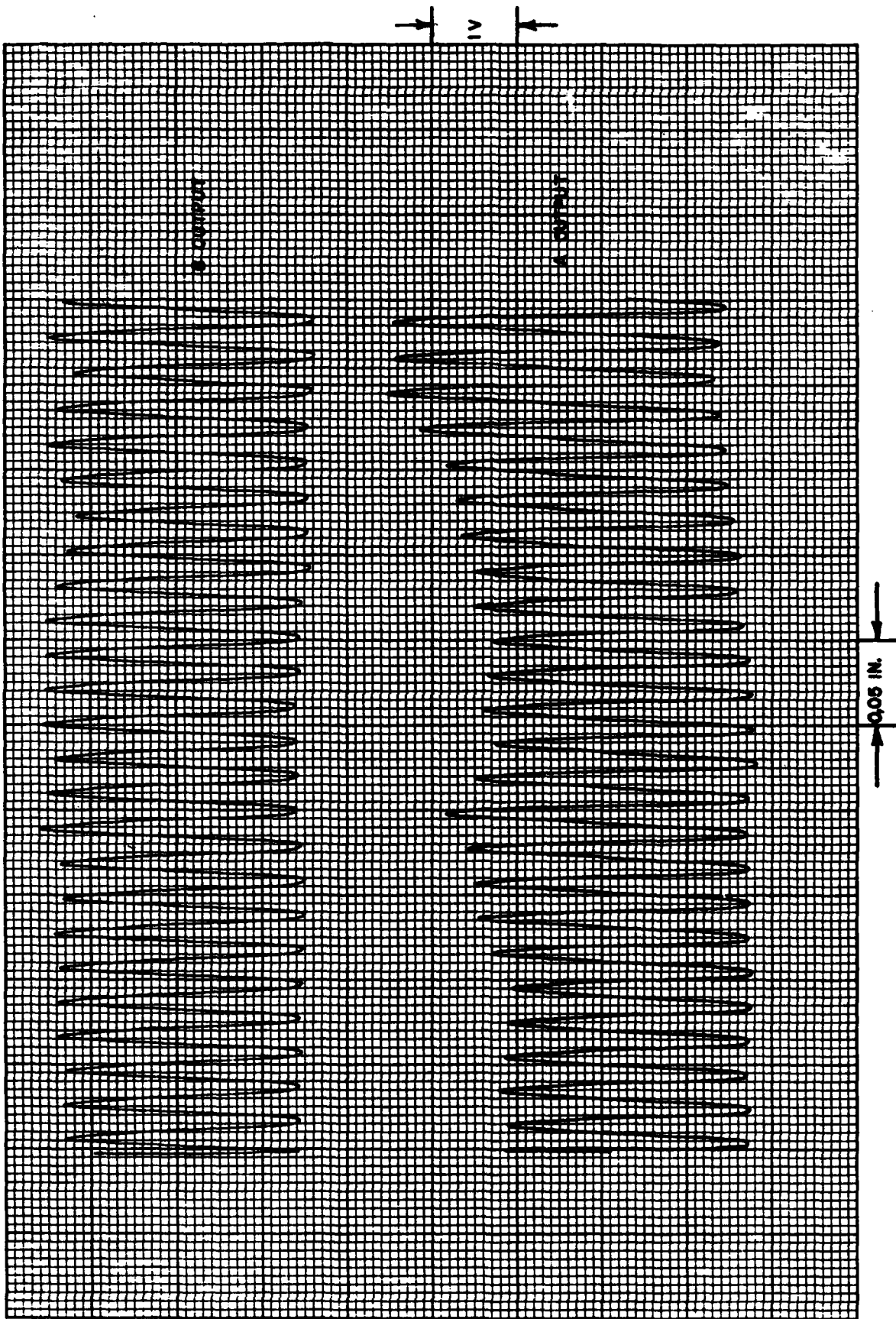


Figure 19 Sensor Output DC Shift

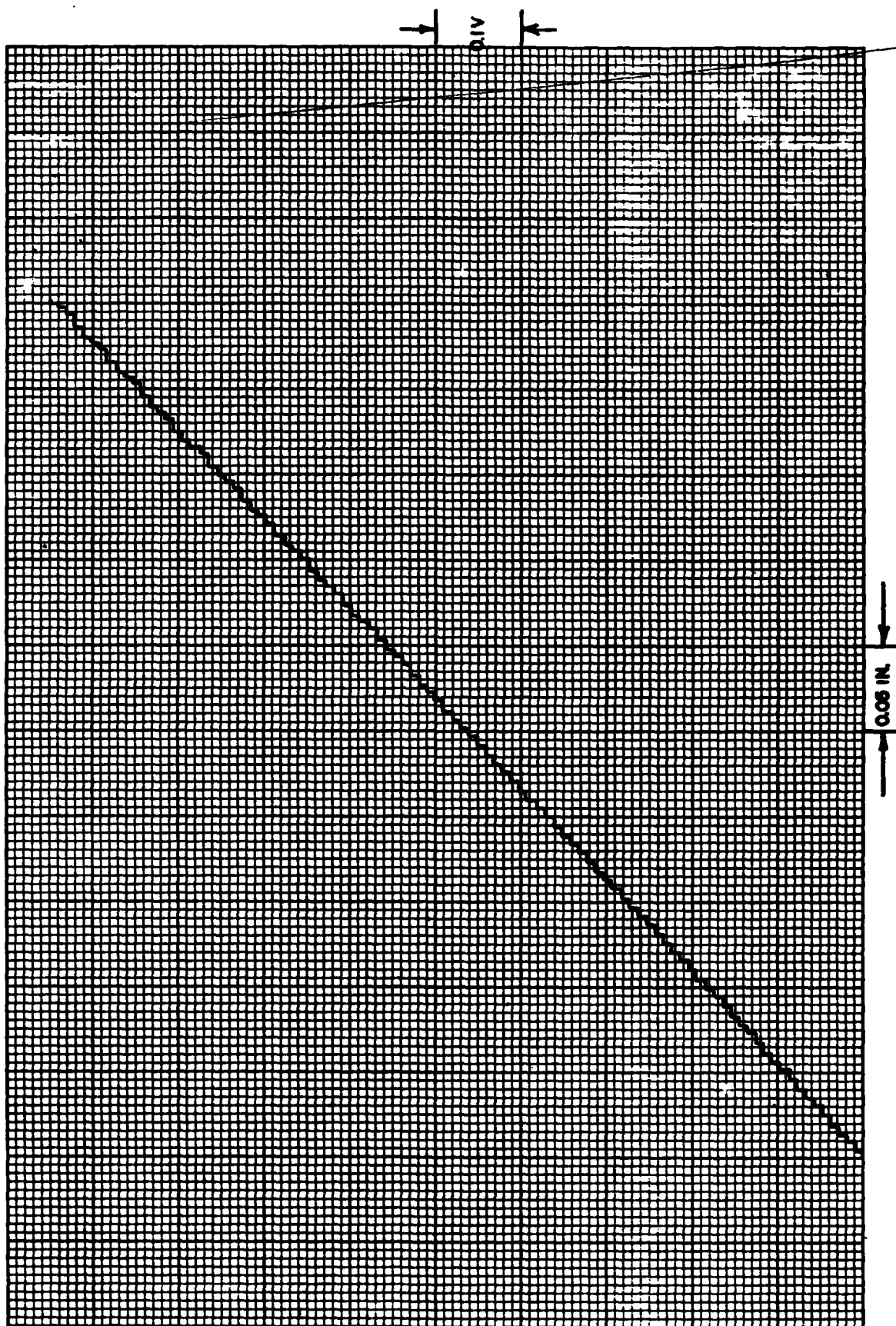


Figure 20 4X Output Linearity without DC Tracking

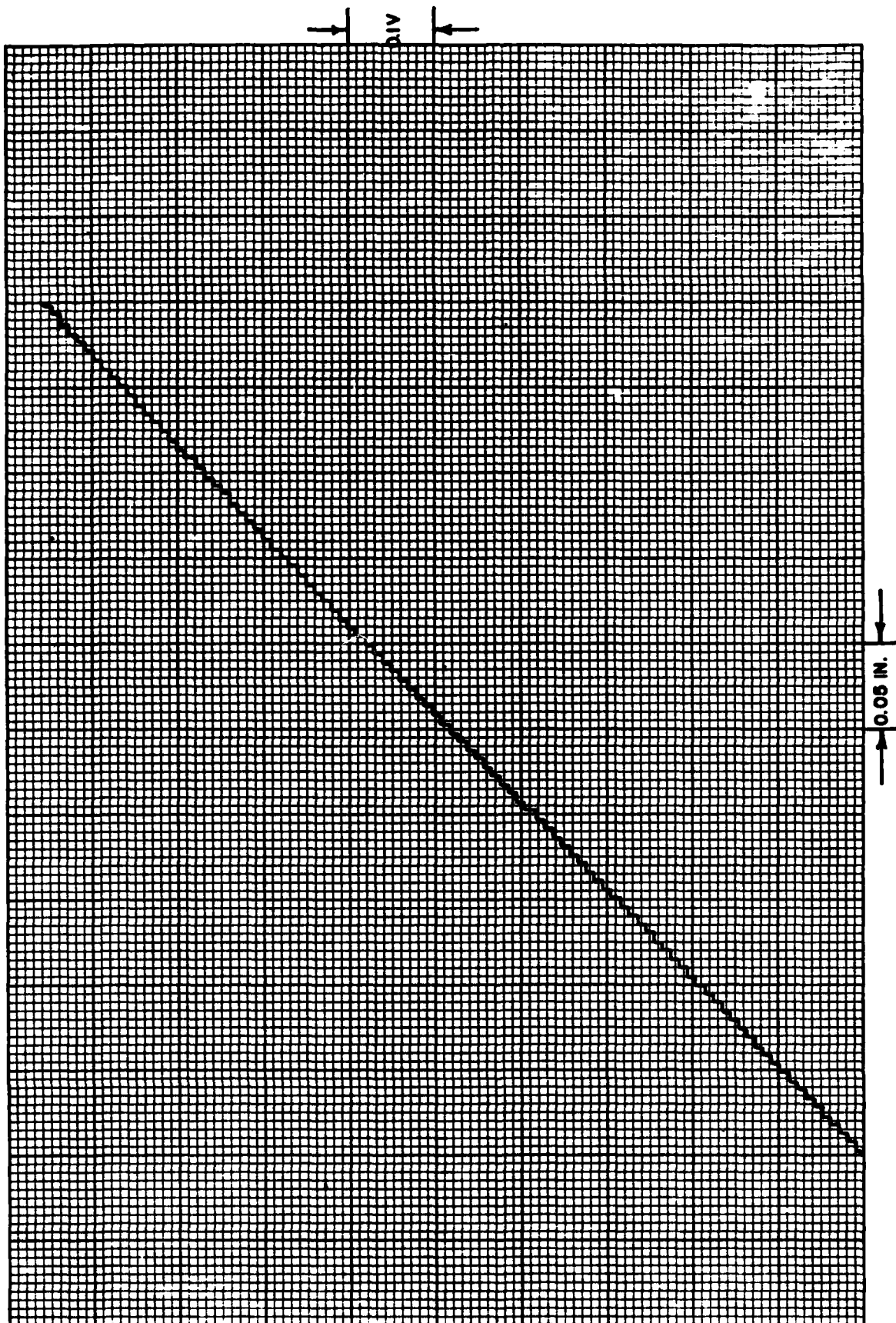


Figure 21 4X Output Linearity with DC Tracking



Figure 22 shows an expanded plot of the 4X output over a deflection of 0.050 in. (this is 10% of the encoded shaft stroke displayed on Figure 22). The shaft movement variation between output changes is a maximum of 0.0005 in., which indicates the accuracy of the measurement technique.

Figure 23 is a plot of the output of the BCD to analog converter for the 8X sensor electronics configuration. The configuration uses the DC tracking circuitry. Figure 23 shows the configuration's output for a shaft displacement of 0.500 in. The change in the amplitude of the steps from the output of the BCD to analog converter compared to the 4X configuration (ref. Figure 21) is apparent. Some irregularity in the steps is noticeable, primarily due to the distortion in the sinusoidal waveform from the sensors. Figure 24 shows an expanded plot of the configuration's output over a stroke of 0.050 in. This plot shows more clearly the irregularity in the steps. A straight line has been drawn through the plotted output to show the resolution. The maximum deviation of the BCD to analog converter's output from the straight line output is 0.0025 in..

In addition to the linearity testing, a slew rate test on the 4X configuration was run. The method of testing was to extend or retract the shaft manually as rapidly as possible and check after returning to the starting position for a zero counter reading. A non-zero reading indicates lost pulse counts. The maximum rate achieved manually was 17 inches per second (limited by the operator). No lost pulse counts occurred up to this rate. The maximum slew rate is theoretically limited by the excitation frequency of the sensing head. For example, for the 0.010 in. washers, the shaft's slew rate for 5K Hz output from the sensor is 100 in./sec. (one cycle per .020 in. of movement). For a more practical output frequency of 1 Kz, the corresponding slew rate is 20 in./sec.

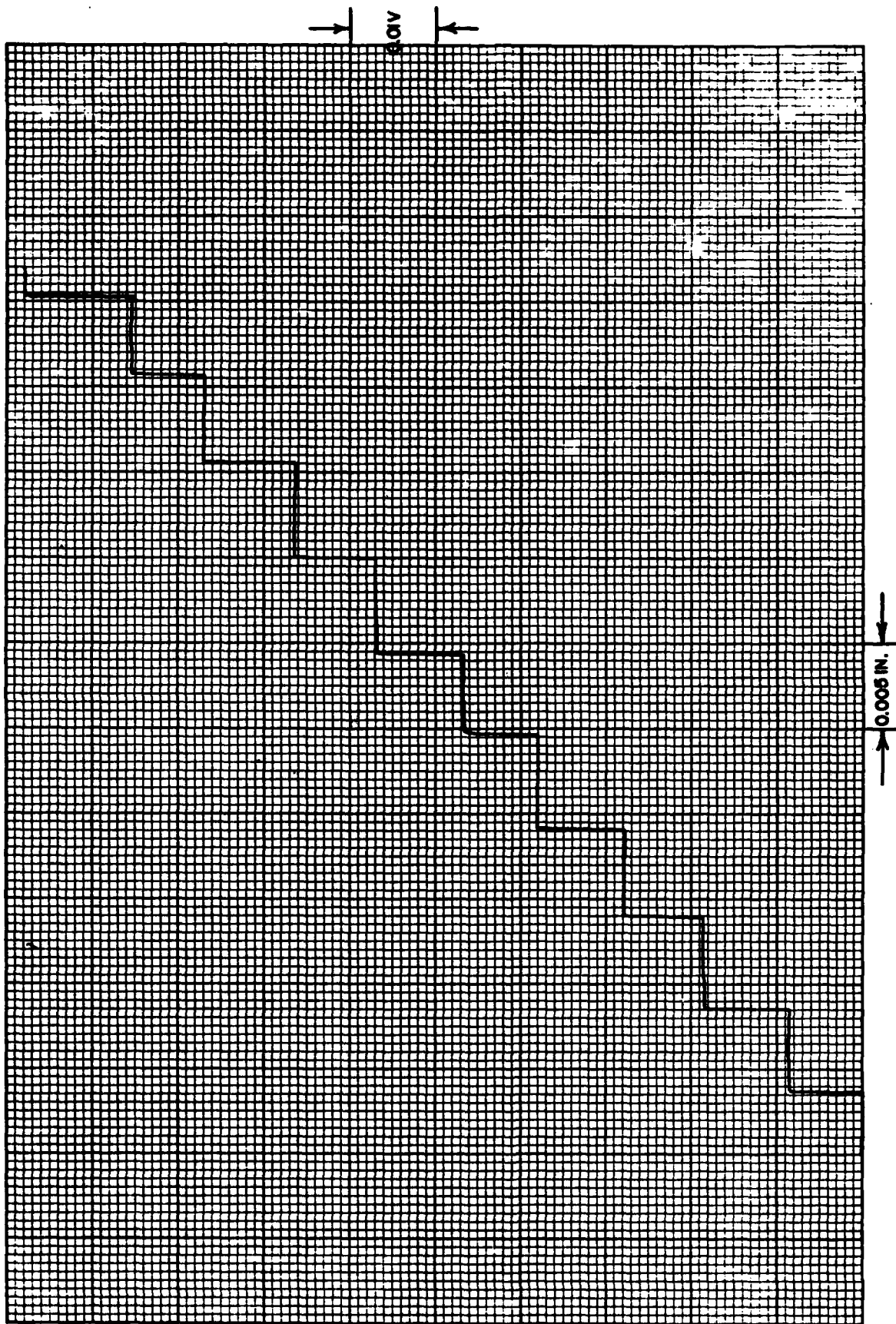


Figure 22 4X Expanded Plot with DC Tracking

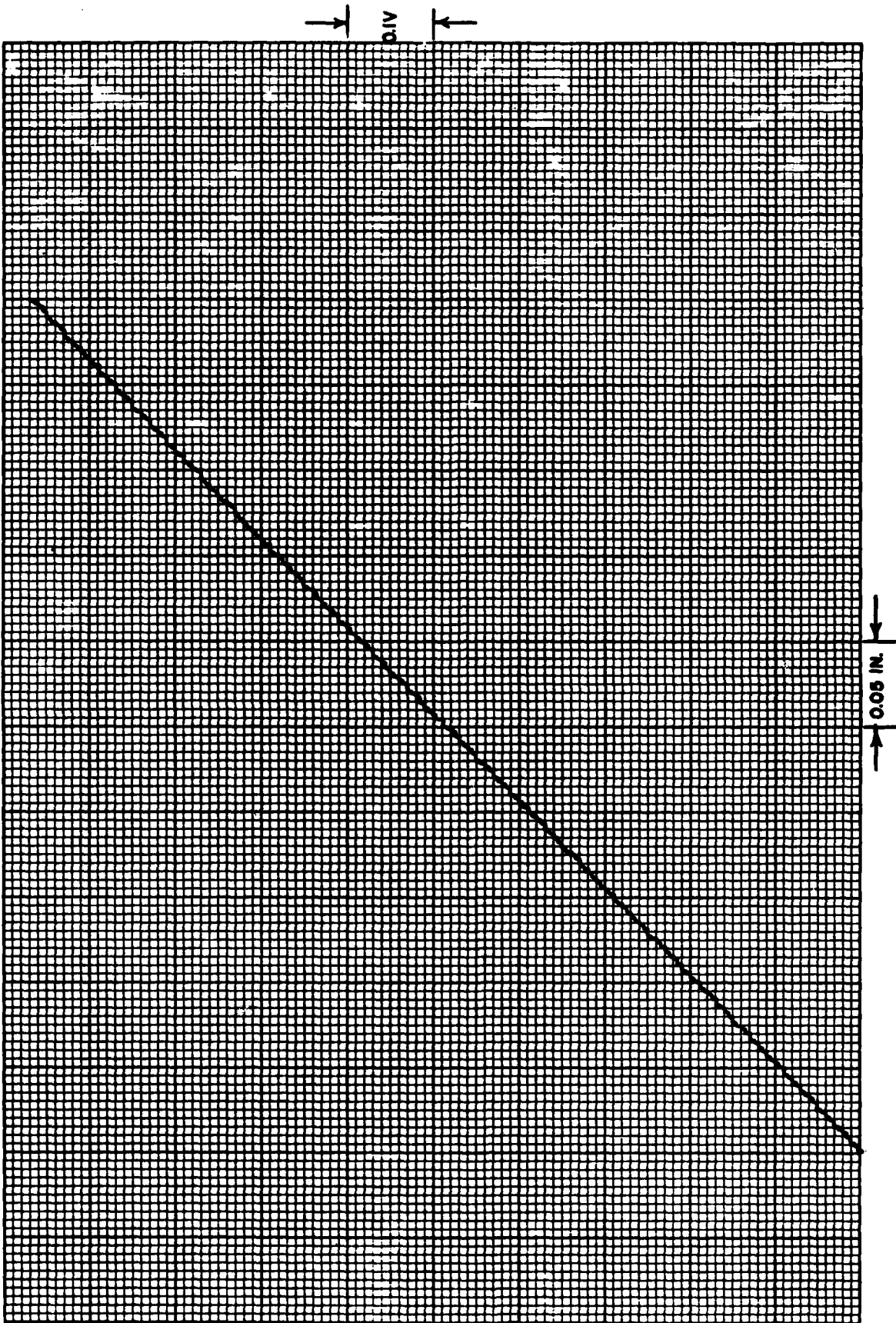


Figure 23 8X Output Linearity

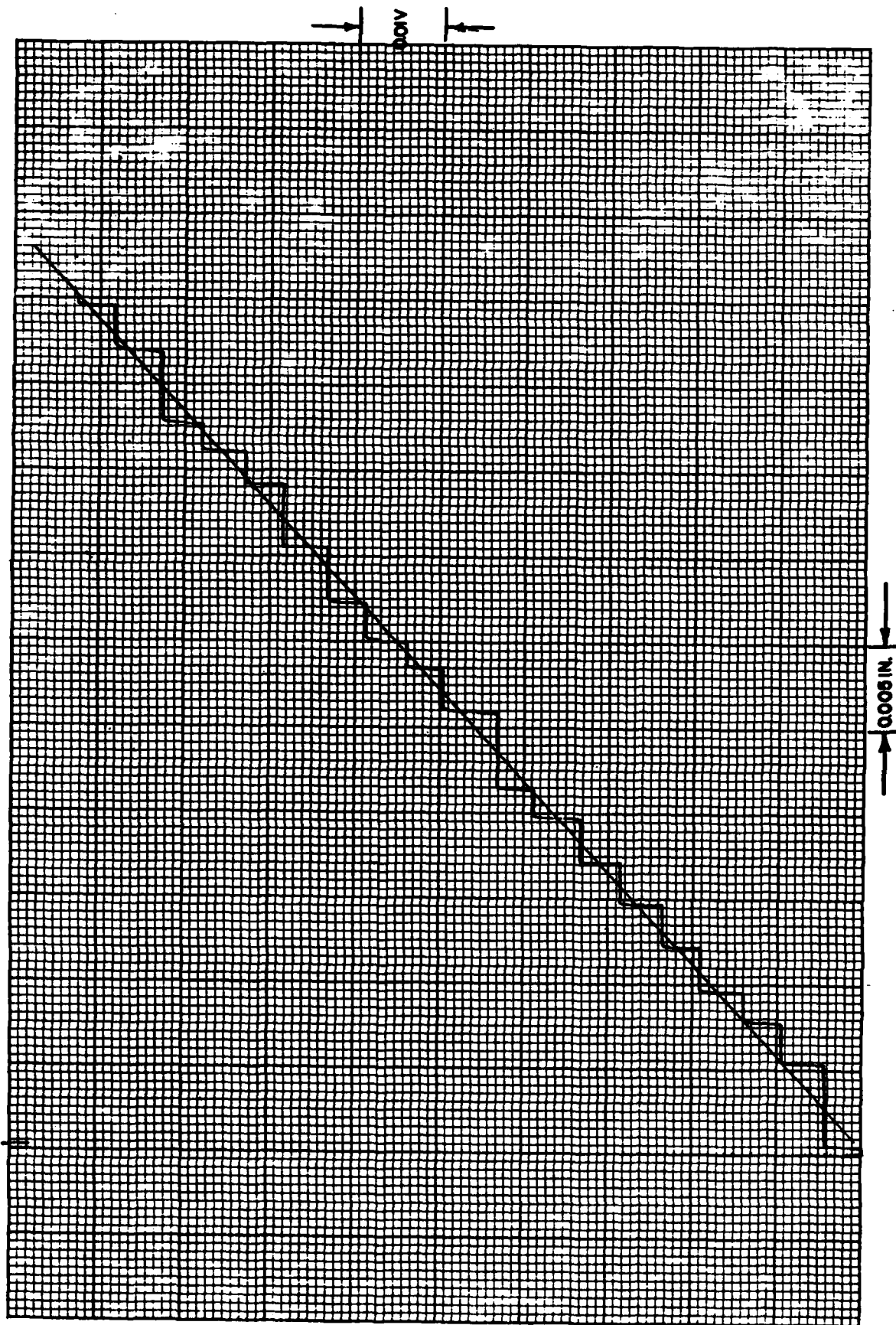


Figure 24 8X Expanded Plot

## SECTION IV

### HARDWARE DESCRIPTION

#### General

The hardware generated for the investigation of the position sensor was designed to allow adequate flexibility for modifications and measurement of the performance characteristics of the techniques being evaluated. An attempt was made during the design to keep the narrow gap sensor size and mounting configuration small enough to be compatible with typical flight control actuation applications. The electronics associated with the sensors were designed as laboratory evaluation tools and could easily be reduced in size for flight hardware application.

#### Specific

Figure 25 shows the encoded shaft at close range. The nominal shaft diameter was 1.125 in. The alternating washers were brass and steel, with the brass washers stamped from a die cutter designed by Dynamic Controls, Inc. for producing the washers. The inside diameter of the washers was 0.75 in. and a collar was pressed on the shaft to load the washer stack. For the test shaft, a shaft length of 1.25 in. was encoded with washers. No bonding material was used between the washers on the final test shaft. However, anaerobic adhesive and EA929 epoxy were both tried on two other shaft buildups and appear satisfactory. The outside diameter of the encoded shaft section was ground between centers to provide a round and concentric diameter.

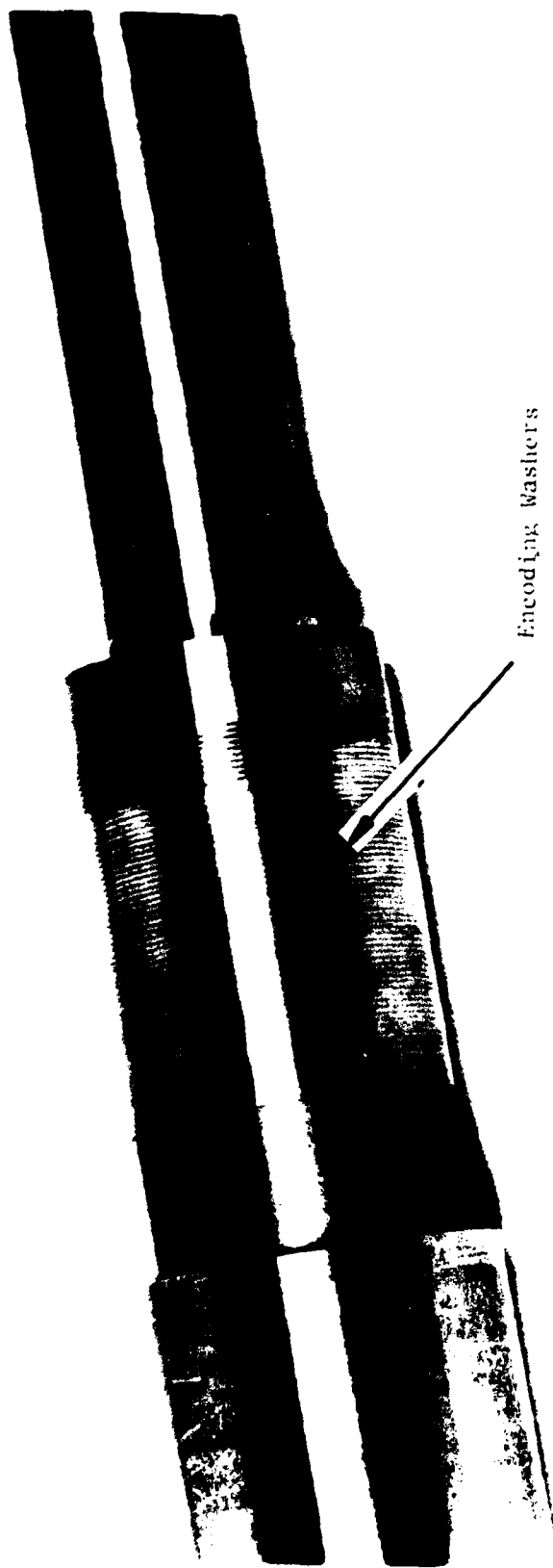


Figure 25 Encoded Shaft Closeup View

For some applications, to prevent corrosion and provide a wear surface for seals, the outside diameter of the washer stack could be chromium plated and ground. The primary limitation would be the thickness of chromium that could be used without decreasing significantly the sensitivity of the sensing head. Thicknesses greater than 0.003 in. may present a sensitivity problem.

Figure 26 is a close up view of a narrow gap sensor positioned over the encoded section of the test shaft. The view was taken during the initial sensitivity testing for the different configurations. The epoxy used to bond the two halves of the transformer together and the primary and secondary windings are apparent in the figure.

Figure 27 shows the test setup used during the sensitivity testing. A Wavetech function generator was used to excite the primary winding of the narrow gap sensor being evaluated. The oscilloscope at the right of the Figure 27 was used to measure the secondary winding's output characteristics. The electronics box immediately behind the test shaft was used to amplify and filter the output of the secondary winding. Note that the test shaft assembly uses linear ball bushings to support the encoded shaft. A micrometer head mounted at the right end of the test shaft is used to move the shaft. A coil spring at the left end of the shaft mounting assembly is used to maintain the shaft in contact with the micrometer head. A magnetic mount for a dial indicator was used to position the sensing head for the technique being evaluated. This mount allowed easy variation of the spacing and angular orientation of the sensor to the encoded shaft.

Figure 28 is a closeup end view of the sensor ring used to mount the narrow gap transformers around the encoded shaft. Note the four sensor gap ends located



Figure 26 Narrow Gap Transformer Sensor and Encoded Shaft



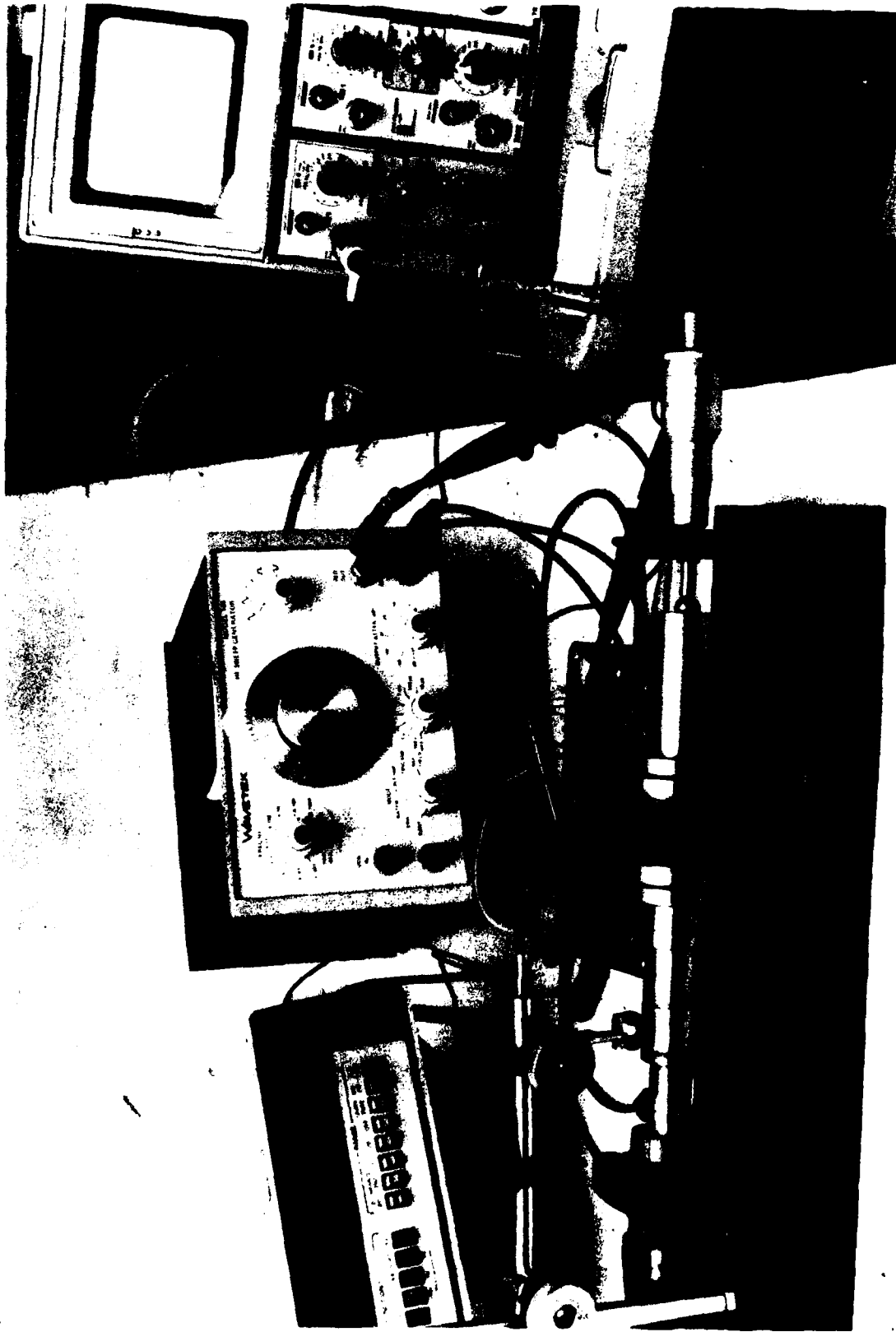


Figure 27 Sensor Sensitivity Test Setup

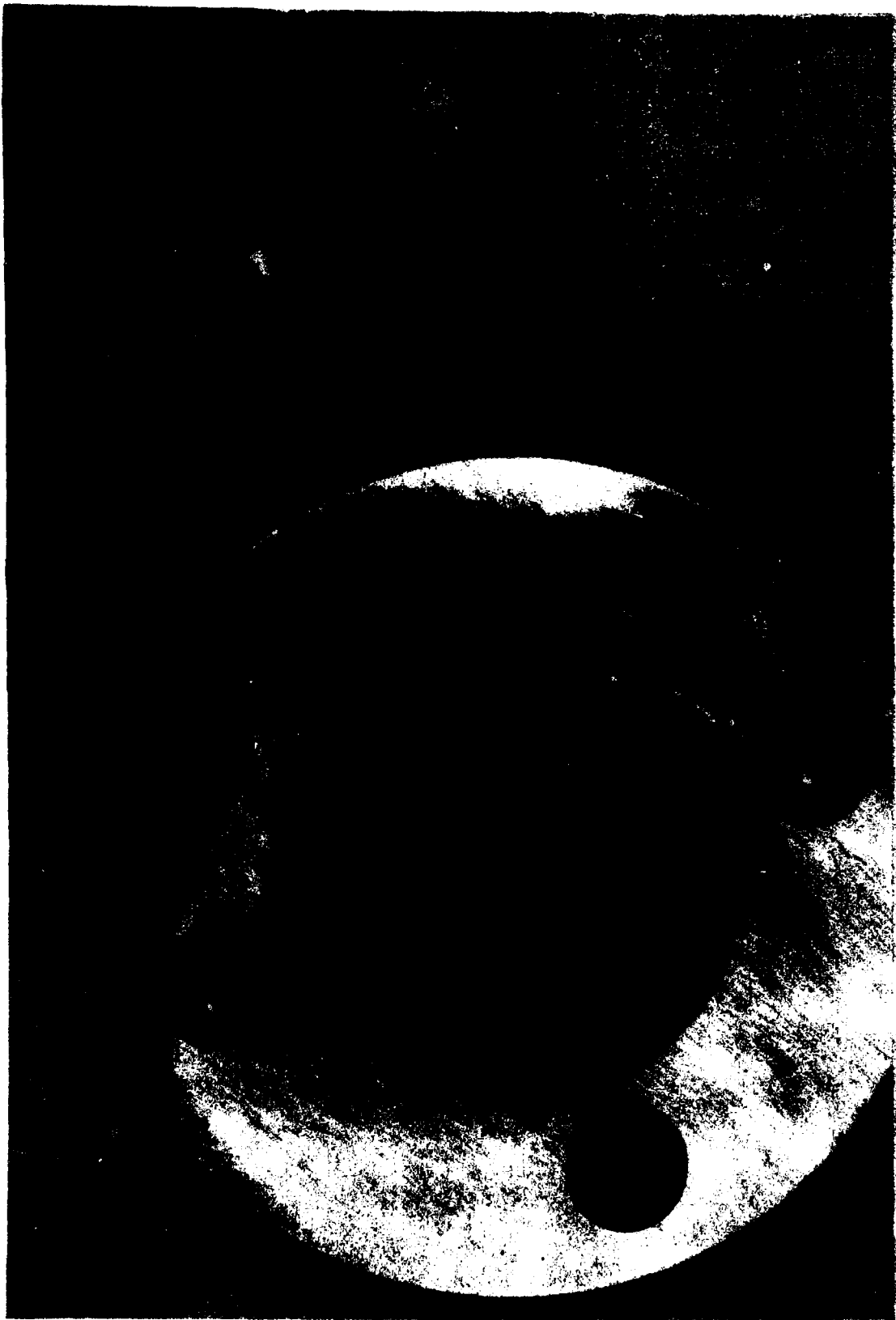


Figure 28 Sensor Ring Assembly-End View

at 90° intervals around the inner circumference of the ring assembly. Figure 29 shows the internal construction of the sensor mounting ring. The transformers were retained by an aluminum ring with recesses machined to match the transform core dimensions. As part of the development of the narrow gap sensor, the ring mount was modified to include alignment set screws for each transformer. The set screws were installed to allow both lateral (along the shaft) motion in order to establish the sensor head offset needed and rotation (to trim the head gap to be parallel to the plane of the encoding washers). The trimming affected the sensor output waveform and was required for satisfactory operation of the 8X configuration. Note that as shown on Figure 29, two transformer pairs are used, one pair for each sensor output. The transformers for each pair are mounted directly opposite each other to minimize the effects on the sensor outputs of encoded shaft to support bearing clearances and eccentricity in the encoded shaft or bearings.

Figure 30 shows the circuit card constructed for the electronics which generated the 10K Hz excitation for the narrow gap transformer primary windings. The two cylindrical components at the left side of the board are the power transistors for driving the primary windings. Figure 31 show the secondary winding signal conditioning and logic circuit board for the 4X configuration. Figure 32 shows the internal construction of the electronics unit with the primary and secondary winding circuit boards installed. Also installed in the unit are the power supplies, the BCD to analog converter and the digital voltmeter. Figure 33 shows the front of the electronics unit. Two digital displays are used, one for analog output voltage of th BCD to analog converter and the other the output of the up/down counter. The reset switch to the right of the readouts is used to initalize the logic circuits upon startup.



Figure 29 Sensor Mount

Sensor A Transformer Pair

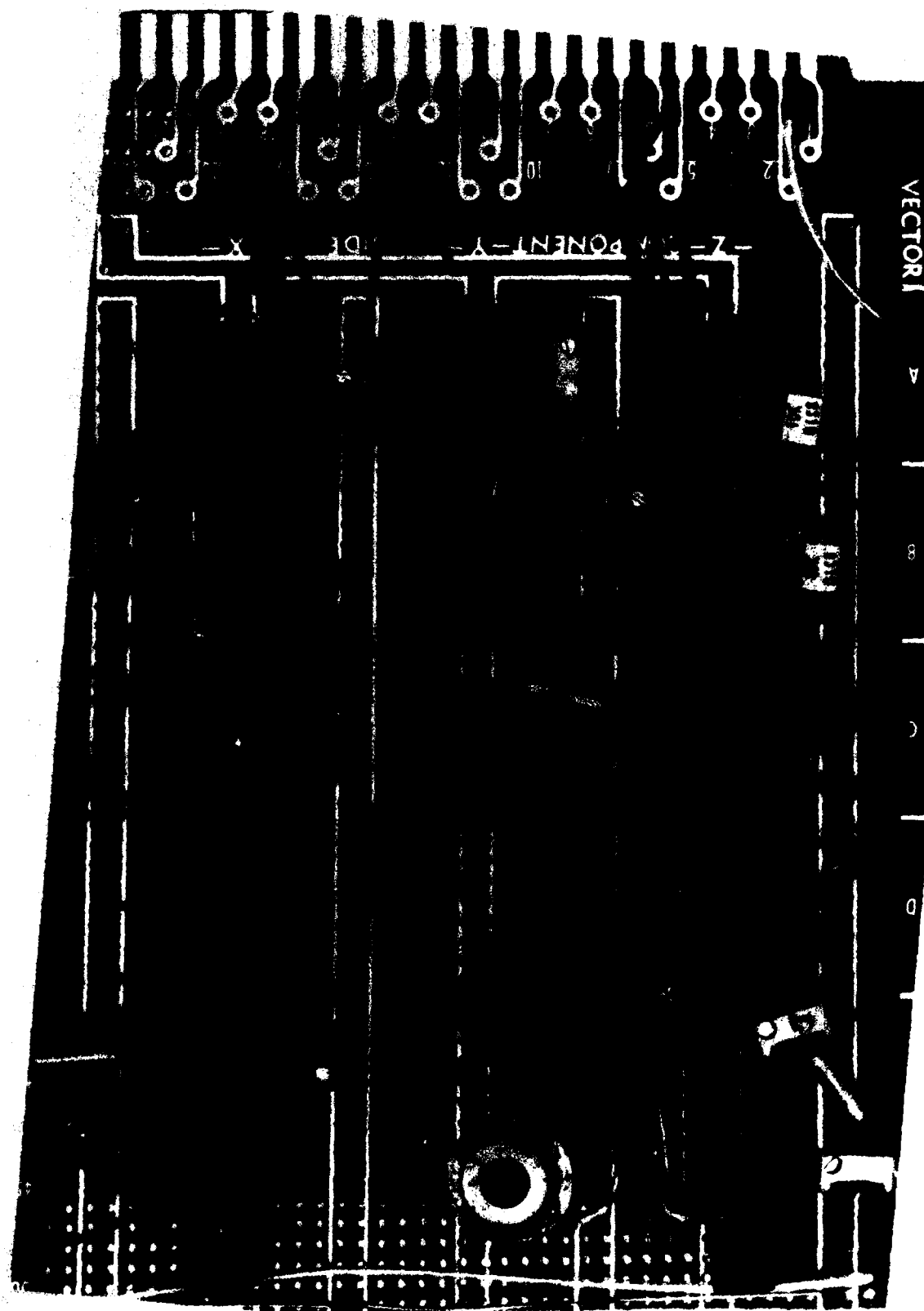
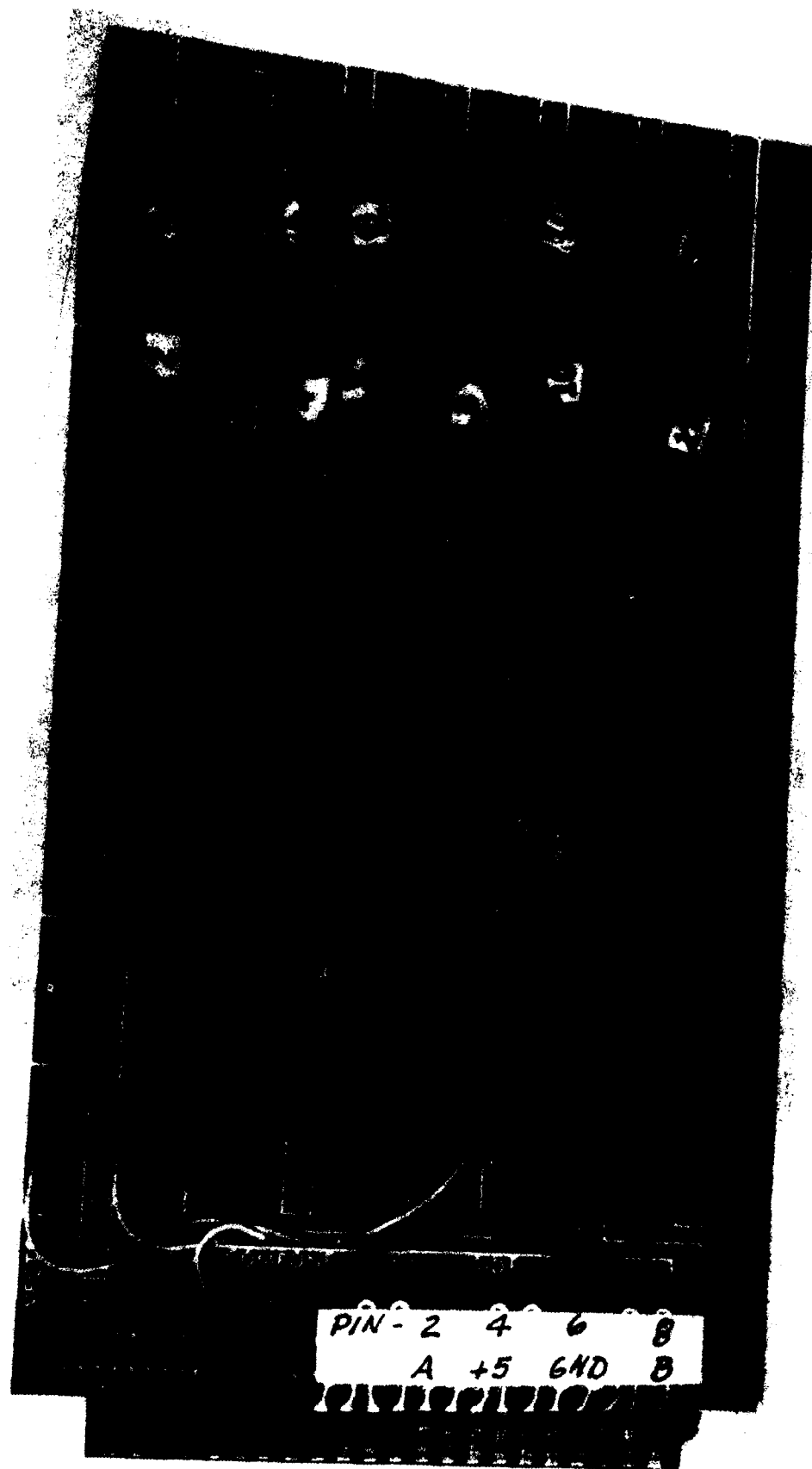


Figure 30 Position Sensor Transformer Primary Circuit Card



PIN - 2 4 6 8  
A +5 GND 0

Figure 31 Position Sensor Transformer Secondary Circuit Card

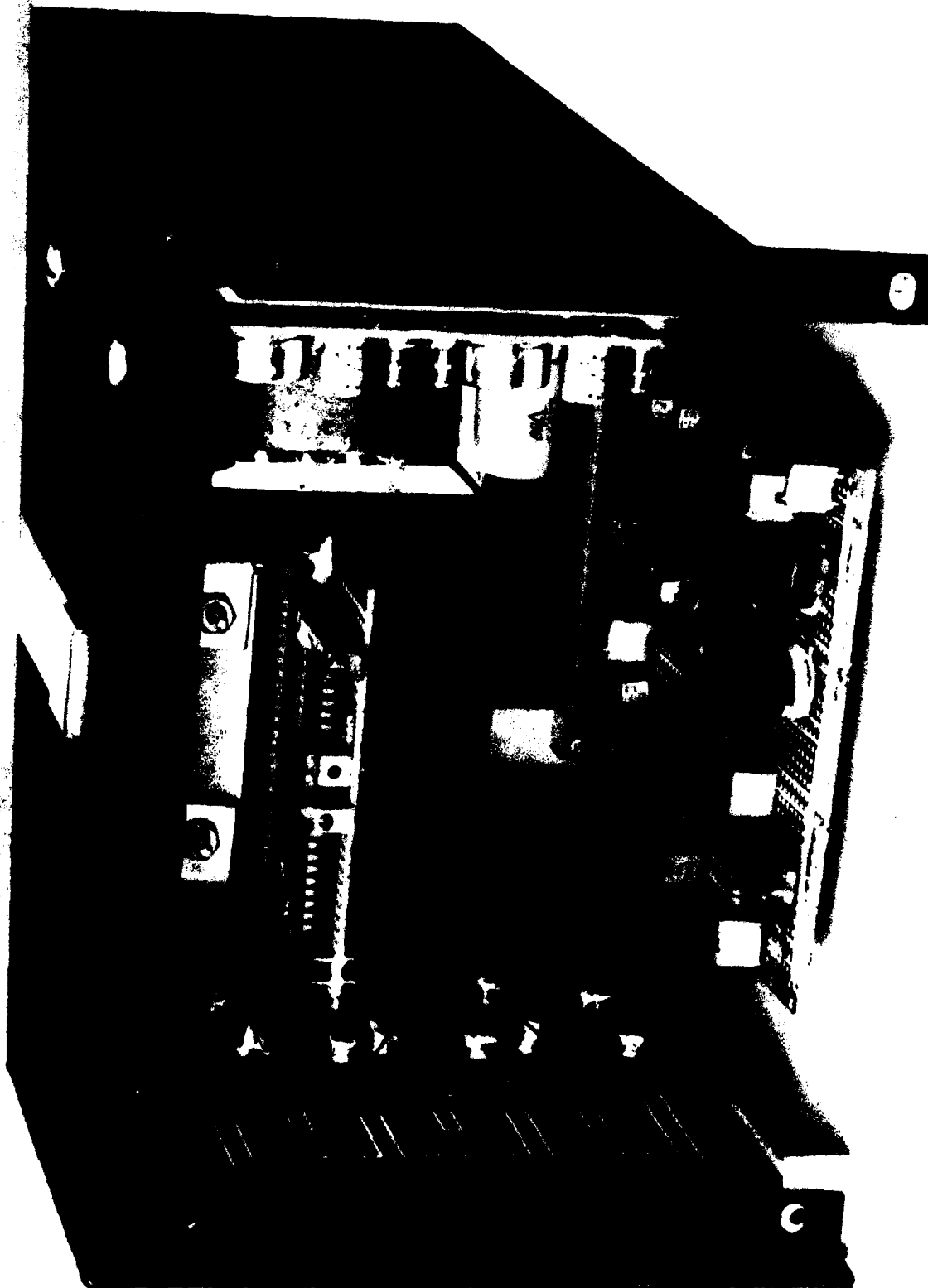


Figure 32 Position Sensor Electronics Unit-Internal View

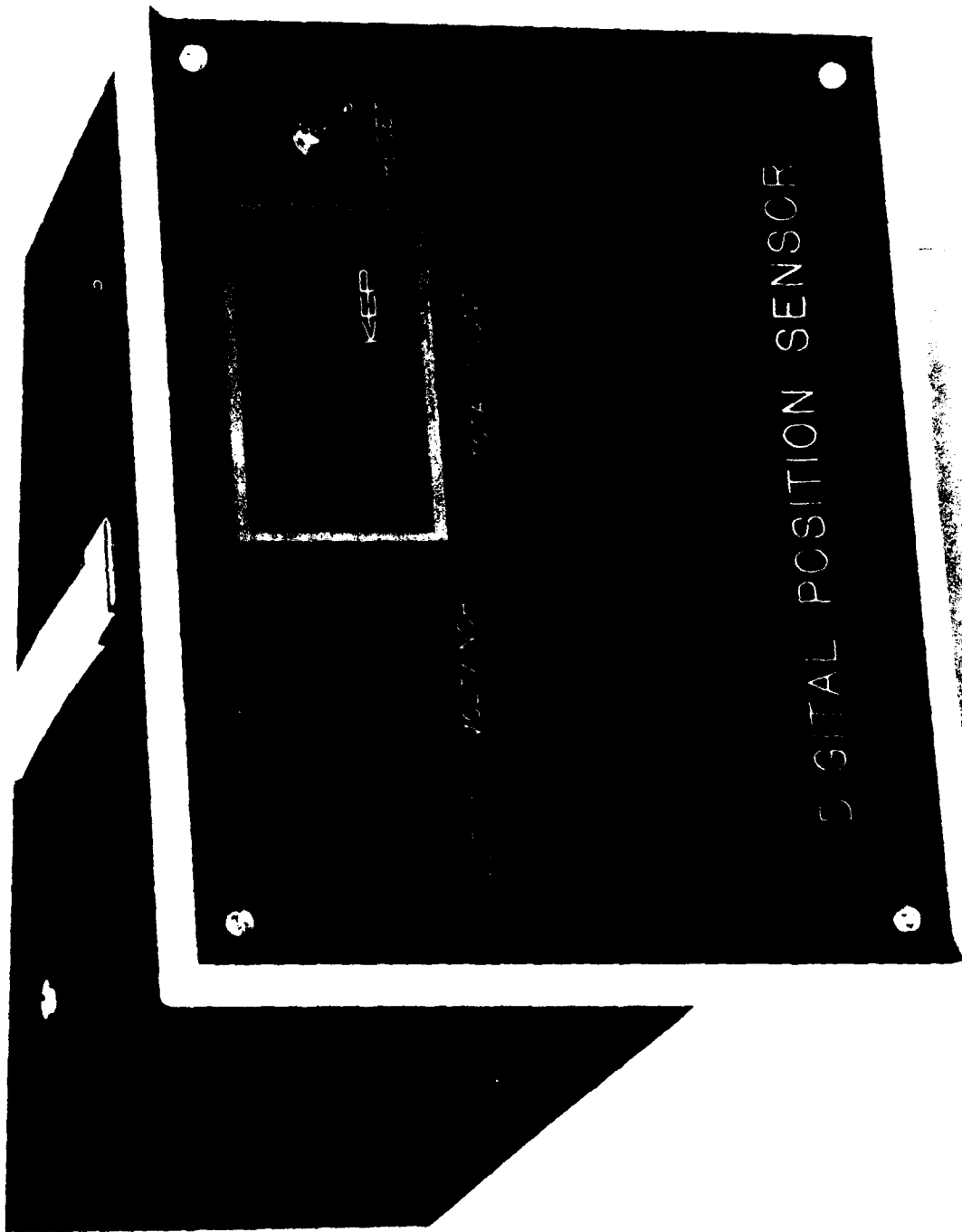


Figure 33 Position Sensor Electronics Unit



SECTION V  
CONCLUSIONS AND RECOMMENDATIONS

Conclusions

The narrow gap sensor technique investigated works well enough to warrant further development. However, the sensitivity of the narrow gap transformer is considerably less than that calculated. This is probably due to the fringing effect of adjacent encoding washers reducing the reluctance change at the gap of the sensor from that predicted by calculations using one washer.

The narrow gap transformer technique requires that the sensing head be fabricated with good precision. The techniques for doing this (and making the sensing head smaller) are already established for the tape recorder manufacturing industry. There should be no difficulty in producing sensing heads with gaps down to 1/10th the gap used for the investigation hardware. A smaller gap would be required if thinner washers were used to encode the shaft.

The 8X logic configuration worked with the demonstration hardware and can produce resolutions of 0.0025 in. for a shaft encoded with 0.010 in. thick washers. However, the requirement for an output waveform having a consistent gradual transition from the sensor's minimum output level to maximum output level makes trimming of the sensor alignment critical. To achieve the same resolution, the 4X logic configuration with a requirement for only consistent zero level crossing could be used with 0.005 in. thick encoding washers and smaller sensor gap.

The DC tracking electronics circuitry worked well for the 4X logic configuration and was required in order for the 8X logic configuration to function. This circuit configuration has general application potential for any decoding scheme where DC shifts of a measurement signal need to be actively compensated. The primary limitation of the particular circuit used with the narrow gap sensor is the sample and hold stability with time. A time period greater than 15 minutes with no shaft movement (and no new samples) could cause a droop in the sampler's output voltage and miscounting. However, if the sampled values were loaded into digital memory, then the time limitation is removed.

#### Recommendations

The sensor mechanization has sufficient promise to recommended further development, particularly in the following areas:

1. Improvement of the narrow gap transformer sensitivity
2. Improvement of the resolution with thinner encoding washers
3. Evaluation of the effect of chromium plating over the encoding washers on the sensitivity of the sensors
4. The incorporation of additional sensing assemblies in order to achieve sensor output redundancy using the same encoded shaft

END

FILMED

9-84

DTIC